

Land cover change impacts on atmospheric chemistry: simulating projected large-scale tree mortality in the United States

Jeffrey A. Geddes¹, Colette L. Heald², Sam J. Silva², and Randall V. Martin^{1,3}

[1]{Department of Physics and Atmospheric Science, Dalhousie University, P.O. Box 15000, Halifax, Nova Scotia, B3H 4R2, Canada}

[2]{Department of Civil and Environmental Engineering, Massachusetts Institute of Technology, 77 Massachusetts Avenue, Cambridge, Massachusetts, 02139-4307, USA}

[3]{Harvard-Smithsonian Center for Astrophysics, Cambridge, Massachusetts, USA}

Correspondence to: J.A. Geddes (jeff.geddes@dal.ca)

Abstract

Land use and land cover changes impact climate and air quality by altering the exchange of trace gases between the Earth's surface and atmosphere. Large-scale tree mortality that is projected to occur across the United States as a result of insect and disease may therefore have unexplored consequences for tropospheric chemistry. We develop a land use module for the GEOS-Chem global chemical transport model to facilitate simulations involving changes to the land surface, and to improve consistency across land-atmosphere exchange processes. The model is used to test the impact of projected national-scale tree mortality risk through 2027 estimated by the 2012 USDA Forest Service National Insect and Disease Risk Assessment. Changes in biogenic emissions alone decrease monthly mean O₃ by up to 0.4 ppb, but reductions in deposition velocity compensate or exceed the effects of emissions yielding a net increase in O₃ of more than 1 ppb in some areas. The O₃ response to the projected change in emissions is affected by the ratio of baseline NO_x:VOC concentrations, suggesting that in addition to the degree of land cover change, tree mortality impacts depend on whether a region is NO_x-limited or NO_x-saturated. Consequently, air quality (as diagnosed by the number of days that 8-hr average O₃ exceeds 70 ppb) improves in polluted environments where changes in emissions are more important than changes to dry deposition, but worsens

1 in clean environments where changes to dry deposition are the more important term. The
2 influence of changes in dry deposition demonstrated here underscores the need to evaluate
3 treatments of this physical process in models. Biogenic secondary organic aerosol loadings
4 are significantly affected across the US, decreasing by 5-10% across many regions, and by
5 more than 25% locally. Tree mortality could therefore impact background aerosol loadings by
6 between 0.5 to 2 $\mu\text{g m}^{-3}$. Changes to reactive nitrogen oxide abundance and partitioning are
7 also locally important. The regional effects simulated here are similar in magnitude to other
8 scenarios that consider future biofuel cropping or natural succession, further demonstrating
9 that biosphere-atmosphere exchange should be considered when predicting future air quality
10 and climate. We point to important uncertainties and further development that should be
11 addressed for a more robust understanding of land cover change feedbacks.

12

13 **1 Introduction**

14 Land use and land cover changes impact climate by altering energy exchange at the surface of
15 the Earth, and by altering the composition of the atmosphere through changes in
16 biogeochemical cycling (Feddema et al., 2005; Pielke et al., 2011). Though recognized as a
17 crucial factor in future climate scenarios (van Vuuren et al., 2011), projections of land use and
18 land cover change remain highly uncertain (Smith et al., 2010). The terrestrial biosphere also
19 plays an important role in surface-atmosphere exchange of reactive trace species that control
20 the oxidative chemistry of the troposphere (Arneth et al. 2010; Laothawornkitkul et al. 2009;
21 Mellouki et al. 2015; Monson and Holland, 2001), so that changes in vegetation can further
22 impact air quality and climate (Heald and Spracklen, 2015; Unger, 2014). These changes can
23 be human-driven (e.g. urbanization, forestry management, and agricultural practices) or
24 natural (e.g. wildfires, insect infestations, and biome shifts). Over the 21st century, variations
25 in biogenic volatile organic compound (BVOC) emissions due to climate change and crop
26 management will likely impact surface ozone (O_3) and secondary organic aerosol (SOA)
27 concentrations (Ashworth et al., 2012; Chen et al., 2009; Ganzeveld et al., 2010; Hardacre et
28 al., 2013; Heald et al., 2008; Wu et al., 2012). Here we consider the air quality and
29 atmospheric chemistry implications of another form of land cover change on relatively shorter
30 timescales: large-scale insect- and disease-driven tree mortality.

31 Modifications to vegetation distribution, plant type, canopy characteristics, and soil properties
32 alter the regional emission and deposition of reactive trace gases from the terrestrial

1 biosphere. For example, large-scale deforestation of the Amazonian rainforest, the expansion
2 of oil palm plantations in Asia, and cultivation of biofuel feedstocks can significantly alter
3 BVOC emissions, with various implications for secondary pollutants (Ashworth et al., 2012;
4 Beltman et al., 2013; Ganzeveld, 2004; MacKenzie et al., 2011). In the eastern US, harvest
5 practices and forest management have likely resulted in a net increase in BVOC emissions
6 since the 1980s, counteracting successful anthropogenic emission reductions (Purves et al.,
7 2004). Ecological succession, either from anthropogenic land management or natural
8 processes, could also impact regional chemistry (Drewniak et al., 2014). Some changes in
9 land cover have compensating impacts. For example, higher vegetation density could lead to
10 increased O₃ precursor emissions but also faster depositional losses (Ganzeveld et al. 2010;
11 Wu et al., 2012). Consequently, we require models that account for the combination of these
12 mechanisms in a consistent manner to understand the relevant net impacts on air quality and
13 climate.

14 Almost a third of the Earth's land surface is covered by forests, providing a variety of
15 economic, recreational, and ecosystem services including regulating climate through complex
16 biogeophysical and hydrological feedbacks and by taking up CO₂ from the atmosphere
17 (Bonan, 2008; MEA, 2005). A prominent risk to forests in the near future (< decades) is tree
18 mortality resulting from insect attack and disease (Krist et al., 2014). Biotic disturbances
19 resulting in tree mortality occur naturally at low and predictable rates (Smith et al., 2001), but
20 in the coming decades many forests across the US are predicted to experience tree mortality
21 well above background. Between 2013 and 2027, over 80 million acres of treed land in the
22 United States are projected to experience basal area mortality rates exceeding 25%, with some
23 tree species at risk of losing more than 50% of their volume (Krist et al., 2014). The dominant
24 contributing hazards are expected to be root diseases, bark beetles, and oak decline, with
25 highest risks occurring in Idaho, Montana, and Oregon in the western US and in Rhode
26 Island, Connecticut, and Massachusetts in the eastern US (Krist et al., 2014). The wood
27 volume lost from insects and pathogens can cost the US several times more than losses by
28 wildfire (Dale et al., 2001), and can have a major impact on carbon cycling (Hicke et al.,
29 2012), but the atmospheric chemistry impacts have not been fully explored. Berg et al. (2013)
30 simulated the impact of past bark beetle infestations in the western US using a decade of tree
31 mortality data. They found large changes to monoterpene emissions, and subsequently SOA
32 concentrations, that could potentially affect background aerosol concentrations and visibility
33 in pristine regions.

1 Given the important role of natural emissions in the chemistry of the atmosphere (Zare et al.,
2 2014), large-scale future tree mortality may influence ozone production and organic aerosol
3 concentrations. Nonattainment of O₃ air quality standards in the US is more sensitive to
4 BVOC emissions than anthropogenic VOC emissions (Hakami et al., 2006), and secondary
5 organic aerosol mass can be dominated by biogenic sources (Pye et al., 2010). The main
6 anticipated effect of tree mortality is a reduction of the BVOC emissions from the species that
7 die, but a change in local vegetation density would also be expected to impact dry deposition,
8 since this is directly related to the surface area available for deposition. Vegetation changes
9 can also affect the local microclimate, further impacting depositional processes. Changes in
10 dry deposition may be significant for species (such as O₃) whose depositional losses are
11 competitive with chemical sinks near the surface of the earth. Finally, since soil NO_x
12 emissions to the atmosphere depend not only on available nitrogen and soil conditions but
13 also on the extent of uptake to vegetation canopies, changes to forests driven by tree mortality
14 could impact these emissions as well.

15 Here we use the GEOS-Chem chemical transport model to investigate the impact of projected
16 tree mortality on atmospheric composition. We harmonize the description of land cover
17 across the relevant surface-atmosphere exchange processes, and use this adapted model to
18 simulate the impacts of predicted tree losses as a result of insect and disease in the United
19 States from 2013-2027. We explore how changes in dry deposition might compensate for
20 changes in chemical production by separating these impacts in individual simulations. We
21 highlight that even modest tree mortality could impact regional atmospheric chemistry across
22 the US, and identify specific regions for further investigation. We also discuss directions for
23 future development to better understand the influence of vegetation changes on atmospheric
24 reactivity and composition.

25

26 **2 Model description**

27 **2.1 General description of GEOS-Chem**

28 We use the GEOS-Chem model (Bey et al. 2001; www.geos-chem.org) v9-02 to simulate the
29 impact of changes in vegetation on atmospheric chemistry. GEOS-Chem is a global 3-D
30 atmospheric chemical transport model driven by assimilated meteorology from the NASA
31 Global Modeling and Assimilation Office. Our simulations are driven by GEOS-5

1 meteorological data for the year 2010 and performed over North America at the nested
2 horizontal resolution of $0.5^\circ \times 0.667^\circ$, with dynamic boundary conditions supplied from a
3 global simulation at $2^\circ \times 2.5^\circ$.

4 The model includes detailed $\text{HO}_x\text{-NO}_x\text{-VOC-O}_3$ chemical scheme originally presented by Bey
5 et al. 2001. The chemical mechanism includes over 90 species (including the following
6 lumped categories: $>\text{C}_3$ alkanes, $>\text{C}_2$ alkenes, $>\text{C}_4$ alkylnitrates, $>\text{C}_1$ aldehydes, $>\text{C}_1$
7 alcohols, and $>\text{C}_1$ organic acids), over 200 chemical reactions, and over 50 photolysis
8 reactions, incorporating the latest JPL and IUPAC recommendations. Detailed isoprene
9 oxidation chemistry is included, following Paulot et al. (2009a, b) as implemented for GEOS-
10 Chem by Mao et al. (2013). Explicit oxidation pathways are not yet included for terpenes.
11 Given that isoprene dominates biogenic OH reactivity over the continental US, we assume
12 terpenes play a minor role outside of SOA formation (see below) in our land cover change
13 simulations. Gas-aerosol partitioning in the sulfate-nitrate-ammonium system is described
14 according to the thermodynamic ISORROPIA II equilibrium model (Fountoukis and Nenes,
15 2007).

16 Carbonaceous aerosol sources include primary emissions from fossil fuel, biofuel, and
17 biomass burning (Park et al., 2003) and reversible SOA formation following Pye et al. (2010).
18 Secondary organic aerosol are lumped into five species based on the parent hydrocarbons
19 (terpenes, isoprene, light aromatics and intermediate volatile organic compounds, semivolatile
20 organic compounds (SVOCs), and oxidized SVOCs). Aerosol yields are parameterized using
21 a volatility basis set (Donahue et al., 2006) for aerosol systems with multiple parent
22 hydrocarbons or aerosol formation pathways, or an Odum 2-product approach (Odum et al.,
23 1996) for systems with one parent hydrocarbon. Emitted biogenic parent hydrocarbons are
24 lumped in the following manner: (1) α -pinene + β -pinene + sabinene + carene; (2) limonene;
25 (3) t- β -ocimene + myrcene + other monoterpenes; (4) farnesene + caryophyllene + other
26 sesquiterpenes; and (5) isoprene. SOA yields from ozonolysis (at high and low NO_x) and
27 nitrate radical oxidation are represented in the model for groups (1) to (4), while yields from
28 photooxidation (initiated by OH) and nitrate radical oxidation are represented for isoprene.
29 Further gas-aerosol phase coupling occurs for example through N_2O_5 uptake (Evans, 2005)
30 and HO_2 uptake (Mao et al., 2013).

31 We use anthropogenic emission inventories according to the NEI-2005 inventory for the
32 United States (<http://www.epa.gov/ttnchie1/trends/>), CAC for Canada

1 (<http://www.ec.gc.ca/pdb/cac/>), and BRAVO (Kuhns et al., 2005) for Mexico, and scale these
2 to the year 2010 following van Donkelaar et al. (2008). The model also includes biomass
3 burning emissions (GFED3 (Mu et al., 2011)), lightning NO_x (Murray et al., 2012), and
4 volcanic SO₂ emissions (Fisher et al., 2011). Soil NO_x and BVOC emissions are described
5 below.

6

7 **2.2 Default land-atmosphere exchange in GEOS-Chem**

8 Here we briefly describe the main mechanisms in the model by which vegetated land cover
9 impacts atmospheric chemistry.

10 GEOS-Chem v9-02 includes the Berkeley-Dalhousie Soil NO_x Parameterization (Hudman et
11 al., 2012). In this parameterization, the flux of NO_x from soils is a function of temperature,
12 soil moisture, and emission coefficients which depend on available nitrogen and biome type.
13 Biomes (and basal emission coefficients) are defined according to Steinkamp and Lawrence
14 (2011), with 24 different land cover types. Dry spell length is also included to account for
15 pulsing. A canopy reduction factor is calculated according to leaf area index (LAI), wind
16 speed, and surface resistance, and is designed to simulate the uptake of NO_x by vegetation
17 following soil emission (Wang et al., 1998).

18 Biogenic VOC emissions from vegetation are calculated using the Model of Emissions of
19 Gases and Aerosols from Nature (MEGAN v2.02: Guenther et al. (2006), with updates from
20 Sakulyanontvittaya et al. (2008)). In GEOS-Chem v9-02, mapped basal BVOC emission
21 factors are provided as an input to the model and are modulated online by activity factors that
22 are a function of temperature, LAI, photosynthetically active radiation (PAR), and average
23 leaf age.

24 Dry deposition is calculated by the resistance-in-series scheme of Wesely (1989), using a
25 “big-leaf” approximation where the deposition surface is treated as a single uniform surface
26 (or leaf). Dry deposition velocities are calculated as a combination of aerodynamic resistance
27 (R_a), laminar layer resistance (R_b), and surface resistance (R_c). R_a is calculated separately for
28 unstable, moderately stable, and very stable atmospheric conditions, and is a function of
29 roughness heights (which would be a function of land cover type) that are provided by the
30 meteorological input data. R_b depends on meteorological data and the identity of the gas-
31 phase species being deposited. The R_c parameterization depends on the solubility and

1 reactivity of individual chemical compounds and on land type according to Wesely (1989),
2 and is scaled by LAI. Land types are derived by the USGS global land characteristics
3 database (http://edc2.usgs.gov/glcc/globdoc2_0.php), known also as the Olson Land Map).
4 Over 70 land types are represented and mapped to the 11 deposition surface types given by
5 Wesely (1989). Aerosol deposition is also parameterized by the resistance-in-series scheme
6 according to Zhang et al. (2001), with deposition to snow/ice as presented by Fisher et al.
7 (2011). Gravitational settling of dust and sea salt is described according to Fairlie et al. (2007)
8 and Alexander et al. (2005) respectively.

9 As described above, the parameterizations of soil NO_x emissions, BVOC emissions, and dry
10 deposition all depend on LAI in some way. By default, GEOS-Chem uses a MODIS-derived
11 monthly LAI product (Myneni et al., 2007) that is mapped to the GEOS-Chem grid (year-
12 specific or a climatology), and linearly interpolated to daily values.

13

14 **2.3 Modifications to land-atmosphere exchange in GEOS-Chem**

15 Here we document the development of a land use module to describe land-atmosphere
16 exchange in GEOS-Chem and to facilitate simulations involving changes in land cover and
17 land use, such as the tree mortality being explored here.

18 To increase the flexibility in the BVOC emissions, basal emission factors are now mapped at
19 simulation initialization using input land cover data. As a base input, we use present-day (year
20 2000) land cover from the Community Land Model (CLM) v. 4
21 (<http://www.cgd.ucar.edu/tss/clm/> and Lawrence et al. (2011)). Vegetation is divided into 16
22 plant functional types (PFTs, Table A1) and their fractional coverage is mapped globally at a
23 native resolution of 0.23° x 0.3125°. We incorporate updated emission factors following
24 MEGAN v2.1 (Guenther et al., 2012).

25 We also eliminate the dependence of the dry deposition velocities on the Olson Land Map.
26 Instead, the same PFTs that drive BVOC emissions are mapped directly to the 11 deposition
27 types from Wesely (1989). We replace the roughness heights provided by the assimilated
28 meteorological product with values that are specific to the land cover or plant functional type
29 (Table A1). Furthermore, rather than basing dry deposition on the dominant land type at a
30 certain native resolution, the complete sub-grid fractional coverage of all PFT/land types are
31 accounted for. In this way, deposition in the model should be less dependent of the horizontal

1 resolution of the simulation or land cover data set. For soil NO_x emissions, we map the same
2 set of PFTs to the 24 biomes of Steinkamp and Lawrence (2011) based on plant type and
3 latitude (Fig. A1).

4 To achieve consistency between our land type description and the LAI used in the model, we
5 replace the monthly MODIS-derived gridded LAI with the sub-grid PFT-specific monthly
6 LAI from the CLM4 land cover description, also based on MODIS observations as well as
7 additional cropping data (Lawrence et al. 2011).

8 In this way, BVOC emissions, soil NO_x emissions, dry deposition, and surface roughness are
9 all newly harmonized to the same land cover input and vegetation density. These changes
10 make it possible to alter the specified PFT distributions and/or fractional coverages, and self-
11 consistently investigate the impact on biosphere-atmosphere exchange.

12

13 **2.4 Impact of updates and land use harmonization on GEOS-Chem simulation**

14 Our modifications to GEOS-Chem impact the emissions, deposition, and simulated
15 concentrations compared to the default model, demonstrating the important role of land cover
16 on atmospheric chemistry. GEOS-Chem and other chemical transport models have previously
17 shown a large sensitivity to land cover datasets (Li et al., 2013) and biogenic emission models
18 (Fiore, 2005; Kim et al., 2014; Zare et al., 2012). Globally, we find annual emissions of
19 isoprene decrease by 14% from 531 Tg yr⁻¹ to 459 Tg yr⁻¹ with land use harmonization and
20 updated emission factors. The emissions of some monoterpenes decrease (e.g. β-pinene,
21 limonene, sabinene, and carene by 10% or less; ocimene by 36%), while others increase
22 significantly (α-pinene by 64%, myrcene by 145%). Sesquiterpene emissions increase
23 between 20-60% depending on the species. These changes result from the new maps of PFTs,
24 the updated emission factors from MEGAN v2.1 (Guenther et al., 2012), and the new LAI
25 values used. Our modified global emissions are generally consistent with those for MEGAN
26 v2.1 as formulated by Guenther et al. (2012). For example, our α-pinene emissions increase
27 from 40 Tg yr⁻¹ to 66 Tg yr⁻¹, compared to 66 Tg yr⁻¹ estimated by Guenther et al. (2012).
28 Global soil NO_x emissions, which depend on biome mapping from the PFT dataset and LAI,
29 decrease by 2% (from 9.8 Tg yr⁻¹ to 9.6 Tg yr⁻¹).

1 Figure 1 shows how all of the modifications impact predicted global monthly mean O₃
2 concentrations for August 2010. The spatial agreement between the simulations is very high
3 ($r=0.99$), suggesting that our modifications have not made significant changes to predicted O₃.
4 While the changes that we made to the model were not in principle intended to improve the
5 accuracy of the GEOS-Chem O₃ simulation (rather the priority was to more easily enable
6 land-cover change experiments), the updated land cover data and the new consistency in the
7 descriptions modestly improve the spatial correlation ($r=0.54$ to $r=0.56$) between the
8 simulated and gridded monthly mean O₃ observed over North America, Europe, and other
9 locations worldwide (Evans and Sofen, 2015) for the whole year. The modifications tend to
10 decrease the high O₃ concentrations at midlatitudes of the Northern and Southern
11 hemispheres. In particular, the high summer bias in monthly mean O₃ drops by 0.5-0.9 ppb
12 (e.g. from RMSE=15.6 to RMSE=14.8 in August) while making little difference to winter
13 month O₃ (RMSE changed by < 0.3 ppb).

14

15 **3 Predicted tree mortality in the United States**

16 To simulate national-scale tree mortality across the US, we use projected tree mortality rates
17 from the 2012 National Insect and Disease Risk Forest Risk (NIDR) Assessment for 2013-
18 2027, assembled by the Forest Health Technology Enterprise Team of the United States
19 Department of Agriculture Forest Service (Krist et al., 2014). This assessment includes results
20 from 186 individual insect and disease hazard models. We gridded the 240-m spatially
21 resolved total tree mortality data (<http://www.fs.fed.us/foresthealth/technology/nidrm.shtml>)
22 to the native resolution of the new GEOS-Chem land input file ($0.23^\circ \times 0.31^\circ$) and focused on
23 the conterminous United States. We use this data to contrast atmospheric chemistry before vs.
24 after the change in tree cover.

25 Figure 2 shows the default fractional area covered by the sum of all tree PFT categories, and
26 the resulting loss in tree-covered fractions due to projected mortality after applying the
27 fractional loss from the NIDR. We applied mortality losses predicted by the NIDR to all tree
28 species in a particular input grid box, instead of accounting for losses specific to one plant
29 functional type only. The magnitude and spatial distribution of tree loss is qualitatively
30 consistent with the agent- and species-specific summaries in the NIDR assessment (Krist et
31 al., 2014), since certain PFT categories usually dominate in specific regions or grid boxes. We
32 briefly summarize the major agents driving projected mortality in the NIDR assessment here.

1 In the western US, insects causing evergreen mortality include the mountain, western, and
2 Jeffrey pine beetles, spruce and Douglas fir beetles, the Douglas fir tussock moth, and the
3 Western spruce budworm. In the east, insect-driven evergreen mortality is driven by the
4 Eastern spruce and Jack pine budworm and hemlock woolly adelgid in the north, and the
5 southern pine beetle in the south. Engraver beetles and the balsam woolly adelgid affect
6 evergreens in both the west and east. Deciduous tree mortality is large in the northeast and
7 eastern US, where oak and maple decline is high. Deciduous tree mortality by diseases such
8 as beech bark, oak wilt, and Dutch elm is also large. Aspen and cottonwood declines are
9 significant in the western US and Great Plains. While root diseases, which impact both
10 needleleaf and broadleaf tree categories, represent the largest single agent-level hazard, the
11 impact of all bark beetles together are projected to cause the highest basal area losses (Krist et
12 al., 2014).

13

14 **4 Impact of tree mortality on atmospheric chemistry in the US**

15 We perform four simulations (Table 1) to investigate the role of insect- and disease driven
16 tree mortality on atmospheric chemistry: (1) a base scenario in which the vegetation is not
17 altered; (2) a scenario where the BVOC emissions respond to the scaled tree cover, but where
18 soil NO_x and dry deposition are calculated using the land cover in the base scenario; (3) a
19 scenario where the BVOC and soil NO_x emissions respond to the scaled tree cover, but where
20 dry deposition is calculated using the land cover in the base scenario; and (4) a full tree
21 mortality scenario where the BVOC emissions, soil NO_x emissions, and dry deposition are all
22 calculated using the scaled tree cover. The combination of these simulations allows us to
23 decouple the effects of changing BVOC and soil NO_x emissions from the effects of changing
24 deposition. We focus our analysis on June to August since this is the seasonal peak in impacts
25 of changes in biogenic emissions on O₃ and SOA formation across the United States.

26

27 **4.1 Impacts on biogenic emissions and on deposition velocity**

28 Figure 3 shows the simulated emissions of isoprene, total monoterpenes, and total
29 sesquiterpenes, and the change in emissions due to tree mortality. The impact to total
30 emissions across the US is a 6-7% decrease for isoprene, monoterpenes, and sesquiterpenes,
31 with much larger impacts locally. Over the continental US, isoprene emissions are projected

1 to decrease by more than 5% for more than 25% of the model grid boxes (762 out of a total of
2 2693). The highest relative impact to isoprene emissions occurs in the Rocky Mountain
3 forests of the northwestern US, where mortality is projected to be high. For example, the
4 largest relative decrease occurs in Idaho [46.0°N, 115.3°W] where isoprene emissions
5 decrease by 47% ($1.8 \mu\text{mol m}^{-2} \text{hr}^{-1}$), compared to the base simulation. These pine-, spruce-,
6 and fir-dominated forests of the northwest are relatively low isoprene emitters compared to
7 the deciduous forests of the eastern US. The reduction in mean OH reactivity due to tree
8 mortality-induced isoprene changes in the northwest is $\sim 0.2\text{-}0.5 \text{ s}^{-1}$ at most. In the oak-
9 dominated Ozarks of Arkansas and Missouri [$\sim 36^\circ\text{N}$, 92°W], and the central Appalachian
10 region [$\sim 38^\circ\text{N}$, 81°W], baseline isoprene emissions are an order of magnitude higher; the
11 corresponding reduction in mean OH reactivity due to tree mortality-induced isoprene
12 changes exceeds 3 s^{-1} . The highest absolute impact of mortality on isoprene emissions occurs
13 at the border of West Virginia and Virginia [38.0°N , 80.0°W], where emissions decrease by
14 $8.6 \mu\text{mol m}^{-2} \text{hr}^{-1}$ (relative decrease of 26%).

15 Likewise, the highest relative impacts to total monoterpene and total sesquiterpene emissions
16 occur in the Rocky Mountain forests of the western and northwestern US (the largest relative
17 decrease occurs in Colorado [38°N , 106.7°W] where the monoterpene and sesquiterpene
18 emissions decrease by 48-50%). Significant relative impacts are also predicted in the pine
19 forests of the Sierra Nevada (10-20%). In terms of absolute magnitude, the difference in
20 monoterpene and sesquiterpene emissions is largest in pine-dominated forests of the southern
21 US. The highest absolute impacts in the country occur in eastern Texas [31.0°N 94.7°W]
22 where the monoterpene emissions decrease by $1.4 \mu\text{mol m}^{-2} \text{hr}^{-1}$ (or 22 %), and in Arkansas
23 [33.5°N 92.7°W] where sesquiterpene emissions decrease by $0.4 \mu\text{mol m}^{-2} \text{hr}^{-1}$ (or 18%)
24 compared to the base simulation.

25 Figure 4 shows the baseline emissions of NO_x from soils and the simulated change resulting
26 from tree mortality. The highest soil NO_x emissions occur in the central US where crops
27 contribute significantly to the land cover. Soil NO_x emissions are also appreciable in the
28 needleleaf evergreen forests of the northwest and southern US. These forests map to biomes
29 with high NO_x emission factors (about four times greater than for deciduous biomes),
30 resulting in baseline emissions approaching several $\mu\text{mol m}^{-2} \text{hr}^{-1}$. The relative impact of tree
31 mortality on soil NO_x emissions exceeds 10% in some of these areas (the largest relative
32 difference occurs in western Montana [46°N , 115.3°W] where soil NO_x emissions increase by

1 15%). In projecting changes to soil NO_x emissions, we allow the canopy reduction factor to
2 respond to changes in LAI, but we assume that the tree mortality does not impact the basal
3 soil NO_x emission factors (nor soil temperature or moisture). The increase in net emission
4 therefore arises from a decrease in canopy reduction factor only, representing the impact of
5 less NO₂ uptake by the canopy before export into the lower mixed layer. A better
6 understanding of the canopy reduction factor, and accounting for canopy chemistry, would
7 facilitate a more thorough assessment of these projected increases in soil NO_x emissions.

8 Figure 5 shows the dry deposition velocity of O₃ in the baseline scenario, and the simulated
9 change resulting from tree mortality. In the northeast, where deciduous forests dominate and
10 vegetation is dense, O₃ deposition velocities are highest (0.6-0.7 cm s⁻¹) whereas the
11 deposition velocity over needleleaf forests is lower (0.3-0.4 cm s⁻¹). Lowest deposition
12 velocities occur over the arid and sparsely vegetated regions of the country. Where projected
13 tree mortality is high, O₃ deposition velocity decreases by up to 0.08 cm s⁻¹ due to reduced
14 stomatal uptake and change in roughness height. The highest absolute impact occurs in the
15 eastern US, along the border of Virginia and West Virginia [38.0°N, 80.0°W]. On a relative
16 basis the impact is largest in the northwest (deposition velocity in northern Idaho [47.5°N,
17 116.0°W] decreases by 16%, or 0.06 cm s⁻¹). Spatially, the impact on the deposition velocity
18 for other constituents is similar. For example the deposition velocity of HNO₃ (which is
19 largely limited by aerodynamic resistance instead of surface resistance as in the case for O₃)
20 also decreases in the same regions due to the change in roughness heights in the tree mortality
21 scenario. In this case, decreases in HNO₃ deposition velocity exceeding 20% are predicted in
22 the northwest and eastern US.

23

24 **4.2 Impacts on surface ozone concentrations**

25 Figure 6a shows the June-July-August mean surface O₃ concentrations simulated in the base
26 scenario (Simulation 1). The high concentrations in the western US are consistent with
27 previous work and are a consequence of the elevation and the dry climate resulting in a deep
28 boundary layer and slow deposition velocities (Fiore et al, 2002; Wu et al., 2008). High
29 concentrations are also simulated in the eastern US. Figure 6b shows the change in simulated
30 O₃ concentrations as a result of changes in BVOC and soil NO_x emissions in a tree mortality
31 scenario where deposition is calculated using baseline land cover (Simulation 3 – Simulation

1 1). Changes in soil NO_x emissions alone increase O₃ slightly (Simulation 3 – Simulation 2),
2 but this response is an order of magnitude smaller (or less) than the response to decreased
3 BVOC emissions. The result is a net decrease in O₃ on the order of 0.2-0.4 ppb across a large
4 area of the eastern US and in parts of the northwest and California. The largest change occurs
5 in eastern Texas [32.5°N, 94.7°W] where mean O₃ decreases by 0.44 ppb. Concentrations
6 increase slightly over the Ozarks of Arkansas and Missouri [~36°N, 92°W] and the
7 Appalachian region in West Virginia [~38°N, 81°W].

8 Figure 6c shows the simulated change in surface O₃ due to tree mortality including the impact
9 of changes to dry deposition (Simulation 4 – Simulation 1). The increase in concentrations
10 due to slower deposition velocities counteracts the decrease in O₃ concentrations that result
11 from changes in BVOC emissions alone. In some regions these influences are predicted to be
12 roughly equal so that the net change in O₃ is close to zero. However, in many parts of the
13 country including the northeast (e.g. Vermont, New Hampshire, and Maine), and the
14 northwest (northern Idaho and western Montana), the predicted change in deposition is large
15 compared to the change from emissions alone, resulting in net increases to O₃ approaching 1
16 ppb or greater. Over the central Appalachian region (most notably West Virginia) and Ozarks
17 the predicted change including dry deposition is also very large compared to the small
18 increase from emissions alone. The highest increase in O₃ occurs at the tristate intersection of
19 Kentucky, West Virginia and Virginia [37.5°N, 82.0°W], where mean O₃ is 1.4 ppb higher
20 than in the base simulation. The substantial effect of slower dry deposition underscores the
21 importance of understanding canopy deposition and the potential impact of canopy processes
22 on chemical losses in predictions of land cover change impacts. Given the influence of
23 changes in dry deposition in our simulations, exploring the uncertainties in dry deposition
24 calculations should be a priority for model development.

25 Since regions where the impact on tree cover is largest are heavily forested and removed from
26 pollution sources, they tend to have relatively low NO_x concentrations. In such situations, O₃
27 production is expected to be NO_x-limited so that decreases in VOC emissions weakly impact
28 O₃ formation. This is the case over the central Appalachian and Ozarks regions, where NO_x
29 concentrations are below 1 ppb and BVOC emissions decreased by 10-20%, but where O₃ is
30 minimally impacted in the scenario with altered emissions only (Fig. 6b). In these forest
31 environments, the change to dry deposition velocity will be the dominant mechanism
32 impacting O₃ concentrations, and indeed we find that O₃ increases when all mechanisms are

1 considered (Fig. 6c). On the other hand, in high-NO_x (or polluted) regions, O₃ production can
2 be expected to be more sensitive to changes in VOC emissions, and since these areas tend to
3 be more developed, deposition plays a smaller role. As a result, in the scenario considering
4 only changes in emissions we find that the predicted impact to O₃ concentrations is relatively
5 large in the heavily populated regions along coast of the mid-Atlantic (Fig. 6b, ~40°N, 74°W).

6 In general, we find that the ratio of NO_x to VOC concentrations (ppb NO_x / ppb C) in a grid
7 box can explain some of the O₃ response to changes in tree cover across the US, despite
8 varying degrees of predicted land cover change. Figure 7 shows histograms of the change in
9 surface O₃ concentrations for two populations of grid boxes that had changes in isoprene
10 emissions of at least 0.1 μmol m⁻² hr⁻¹ (N = 1115 grid boxes from a total of 2693 grid boxes in
11 the continental US). These two distributions (N=111 in both) are grid boxes with the lowest
12 10% NO_x:VOC concentrations in the base scenario, and grid boxes with the highest 10%
13 NO_x:VOC concentrations in the base scenario. These distributions are statistically different
14 (p<0.001, Wilcoxon rank-sum test), and represent the general pattern of impact on “clean”
15 and “polluted” regions respectively. The top panel displays results based on the scenario
16 where only biogenic emissions change (Simulation 3 – Simulation 1). Grid boxes with the
17 highest NO_x to VOC ratios tend towards stronger changes in O₃ concentrations than the grid
18 boxes with lowest NO_x to VOC ratios. This suggests more generally that in addition to the
19 extent of land cover change, the impacts of tree mortality on O₃ can depend on whether the
20 conditions are NO_x-limited (low NO_x:VOC) or VOC-limited (high NO_x:VOC). This NO_x-
21 dependence of the regional chemistry impacts resulting from land system changes has also
22 been identified by Wiedinmyer et al. (2006) and Hardacre et al. (2013) for example. The
23 bottom panel displays the results based on the scenario where changes to biogenic emissions
24 and dry deposition are accounted for (Simulation 4 – Simulation 1). Here we find that the
25 change in O₃ is more frequently positive (increasing O₃ compared to the base scenario) in the
26 low-NO_x to VOC grid boxes, since the deposition response tends to be large compared to the
27 impact of emissions. In contrast, while slower deposition counteracts some of the decrease in
28 O₃ concentrations in the more polluted grid boxes, the net impact remains largely negative
29 (decreasing O₃ compared to the base scenario).

30 The changes in monthly mean ozone mask even larger impacts on shorter timescales (hours)
31 that may be of importance to air quality standards. The magnitude of the impact on surface O₃
32 in the scenario that considered changes to both emissions and deposition is highest during the

1 day and less significant at night due to the diurnal pattern of chemical O₃ production and
2 biogenic emissions, and to the strong dependence of modeled deposition velocities on time of
3 day. As a result, the number of days with O₃ above a specific threshold changes in many
4 locations depending on the land cover scenario. We consider for example daily maximum 8-
5 hr averages. The EPA has recently revised the O₃ air quality standard to be based on 8 h
6 averages exceeding a threshold of 70 ppb instead of the previous 75 ppb
7 (http://www3.epa.gov/ttn/naaqs/standards/ozone/s_o3_index.html), so we investigate the
8 number of days during June–July–August in each grid box of the US where the 8 h average
9 O₃ exceeds 70 ppb. In the scenario considering only a change in emissions (Simulation 3 –
10 Simulation 1), the number of days exceeding an 8 h O₃ concentration of 70 ppb decreases in
11 16% of the grid boxes in the lowest NO_x:VOC decile (“clean” regions of the US), and in 45%
12 of the grid boxes in the highest NO_x:VOC decile (“polluted” regions of the US). Across the
13 US, the number of exceedances decreases by 4 or more days in several regions such central
14 South Carolina (34.0° N, 81.3° W), central Kentucky (37.5° N, -86.0° W), central Indiana
15 (38.5, -90.7), northern Ohio (41.5° N, 83.3° W), and southwest Michigan (42.0° N, 71.3° 20
16 W). In the scenario considering both the change in biogenic emissions and also the change to
17 deposition rates (Simulation 4 – Simulation 1), many grid boxes experience a net increase in
18 the number of days exceeding an 8 h O₃ concentration of 70 ppb. The increase impacts clean
19 regions disproportionately (30 % of lowest NO_x:VOC grid boxes) compared to polluted
20 regions (5 % of high NO_x:VOC grid boxes). The largest increase is 4 days, which occurs
21 north of Richmond, VA (38.0° N, 77.3° W). In the same scenario, less than 1 % of the low
22 NO_x:VOC grid boxes experience a decrease in the number of days exceeding an 8 h O₃
23 concentration of 70 ppb, compared to 26 % of the high NO_x:VOC grid boxes.

24 **4.3 Impacts on reactive nitrogen oxide compounds**

25 Figure 8 shows the mixing ratios of reactive nitrogen oxides in the base scenario (Simulation
26 1), and the simulated changes resulting from tree mortality (Simulation 4 – Simulation 1) on a
27 relative scale (% change). We plot the results for the sum of all reactive nitrogen oxides (NO_y,
28 Fig. 8a), in addition to the individual contributions from NO_x (Fig. 8c), HNO₃ (Fig. 8e) and
29 the sum of all alkyl-, peroxy-, and acylperoxy-nitrates (or “organic nitrates”, Fig. 8g). We find
30 that the relative impacts on NO_y and its partitioning as a result of the tree mortality could be
31 locally significant, and are a complex result of all three mechanisms (changes in BVOC
32 emissions, changes in soil NO_x, and changes to the deposition velocities), depending on the

1 chemical species. Total NO_y increases by up to 8% in the northwest (the largest relative
2 increase of 120 ppt is along the Idaho-Montana border [47.5°N, 115.3°W]). The increases
3 here consist of roughly equal increases in NO_x (79 ppt) and HNO_3 (66 ppt) mixing ratios with
4 a smaller decrease in organic nitrates (29 ppt). Over the rest of the country, changes in total
5 NO_y are small, in part because the increases in NO_x and HNO_3 are counteracted by decreases
6 in organic nitrate species. Significant changes in NO_x abundance and NO_y partitioning could
7 alter the transport and removal of O_3 precursors, and alter the peroxy radical chemistry
8 involved in O_3 production.

9 We find that the increases in NO_x are largely a result of elevated soil NO_x emissions
10 (Simulation 3 – Simulation 1). On the other hand, the increases in HNO_3 , which are up to
11 18% on a relative scale, are due to both slower deposition and increasing soil NO_x emissions
12 (Simulation 4 – Simulation 1). Small increases in HNO_3 (locally up to 3-4%) are also
13 observed in the BVOC emissions only scenario (Simulation 2 – Simulation 1). Broad
14 decreases in the organic nitrate concentrations (approaching 10%) are found across large parts
15 of the country. This result is nearly entirely due to the reduction in BVOC emissions alone,
16 with only a small counteracting effect of lower deposition velocities. For example, where the
17 relative impact was largest (a 10% decrease near Missoula MT [47°N, 114.7°W]), the
18 decrease from the BVOC emissions alone is 36 ppt, while the decrease after accounting for
19 dry deposition and soil NO_x emissions is 29 ppt.

20 **4.4 Impacts on organic aerosol**

21 Figure 9a shows the predicted biogenic SOA (BSOA) surface mass concentrations in the base
22 simulation (Simulation 1). The dominant contributors to BSOA over the United States in
23 these simulations are terpenes, consistent with the results of Pye et al. (2010). This results
24 from nitrate radical oxidation included in the SOA mechanism, since terpenes are emitted at
25 night (in addition to during the day) and model aerosol yields from nitrate oxidation are
26 relative high. The baseline simulation predicts BSOA greater than $3 \mu\text{g m}^{-3}$ throughout most
27 of the southeast US, approaching $10 \mu\text{g m}^{-3}$ near the Mississippi-Alabama and Missouri-
28 Arkansas borders. Biogenic SOA contributes 80% or more of the modeled total OA mass
29 concentration in this region and season. In parts of the northeast and on the west coast, BSOA
30 can also exceed $3 \mu\text{g m}^{-3}$ and the model predicts the biogenic contribution to total organic
31 aerosol to exceed 50% there. In the northwest, BSOA approaches $1\text{-}2 \mu\text{g m}^{-3}$.

1 Figure 9b shows the change in BSOA predicted due to tree mortality (Simulation 4 –
2 Simulation 1). In contrast to O₃ and NO_y species (where the relative importance of deposition
3 and chemical production could vary), the simulation predicts consistent decreases in BSOA
4 from the tree mortality scenario as a result of decreasing BVOC emissions. The change in
5 atmospheric lifetime as a result of slower dry deposition is negligible (Simulation 4 –
6 Simulation 3). Across the eastern US, BSOA decreases by 5-10%. The relative impacts are
7 highest where terpene emissions are significant and projected tree mortality is high due to the
8 dominance of terpenes as precursors to BSOA in these simulations. The impact on BSOA due
9 to tree mortality generally exceeds 10% where the contributions of terpene emissions
10 represent 50% or more of total BVOC emissions (in mass carbon). The spatial pattern in
11 Δ BSOA corresponds most to the relative contribution of the lumped MTPA category of
12 terpenes (α -pinene + β -pinene + sabinene + carene). In some parts of the southeast the change
13 exceeds 25% (1-2 $\mu\text{g m}^{-3}$ in terms of absolute mass). The largest absolute impact occurs in
14 southern Arkansas [33.5°N, 92.7°W], where BSOA decreases by 2.0 $\mu\text{g m}^{-3}$ (or 20%). The
15 relative impact is also high in the northwest, where BSOA decreases by 0.5 to 1 $\mu\text{g m}^{-3}$ (the
16 highest relative difference of 39% occurs in northern Idaho [46.0°N 115.3°W]).

17 Given the dominance of BSOA in much of the US, these changes appreciably impact total OA
18 (and consequently total aerosol mass). Relative impacts to the sum of all organic aerosol are
19 on the order of 20% or greater in many parts of the south, northwest, and northern California.
20 These simulations suggest that tree mortality and the concomitant change in biogenic
21 emissions has the potential to impact background aerosol levels by up to 2 $\mu\text{g m}^{-3}$ in some
22 regions. This may be of particular relevance to the EPA Regional Haze Program, aimed at
23 improving visibility in national parks and wilderness areas
24 (<http://www3.epa.gov/visibility/program.html>).

25

26 **5 Discussion**

27 In this study we develop and apply a land use module for GEOS-Chem to demonstrate that
28 projected tree mortality in the coming decades could impact air quality across the US. We
29 find that the changes in BVOC emissions, soil NO_x emissions, and dry deposition can impact
30 O₃ mixing ratios, reactive nitrogen oxide speciation and abundance, and biogenic secondary
31 organic aerosol formation. The magnitude of change in mean O₃ (-0.4 ppb to +1.4 ppb

1 depending on the simulation) and SOA (up to $-2.0 \mu\text{g m}^{-3}$) in some grid boxes is similar to
2 regional changes predicted by examples of biofuel cropping or natural succession scenarios
3 (Ashworth et al. 2012; Porter et al. 2012; Drewniak et al. 2014), and comparable with the tree
4 mortality effect from past bark beetle infestations simulated in western North America by
5 Berg et al. (2013).

6 In the case of O_3 , we find that lower deposition velocities resulting from the change in tree
7 cover could reverse the impact of decreased chemical production. This produces regional
8 variability in the sign of the O_3 response depending on which effect dominates locally.
9 Generally, our simulations predict that high levels of O_3 could be exacerbated in the low- NO_x ,
10 densely forested areas where mortality is projected to be high. This increase in O_3 could have
11 further feedbacks given the documented negative effect of O_3 on forest health (Ashmore,
12 2005; Taylor et al., 1994). Using the number of days when 8-hr O_3 exceeds 70 ppb, we find
13 that tree mortality generally reduces the number of exceedances for high- NO_x environments.

14 Our simulations also predict large impacts on organic aerosol. While the exact yields and
15 SOA composition are uncertain (Hallquist et al., 2009) and depend on the SOA model used,
16 the post-disturbance impact is a robust and direct response to a reduction in biogenic
17 emissions (and is not sensitive to changes in deposition). Similar to the reduction in O_3 that
18 favors polluted regions, the projected tree mortality could decrease background aerosol levels
19 by up to $1\text{-}2 \mu\text{g m}^{-3}$ locally, inadvertently making progress in other air quality objectives (e.g.
20 long-term visibility at National Parks and Wilderness areas where mortality is in some cases
21 projected to be high).

22 These results do not account for changes in anthropogenic emissions that may occur over the
23 same period of time as the changes to vegetation. We therefore performed a subsequent test
24 where the same land cover change was applied, using anthropogenic emissions from 2005
25 (instead scaling the emissions to 2010 as was performed for Simulations 1 to 4). Between
26 2005 and 2010, modeled anthropogenic emissions of NO_x and SO_2 over the continental US
27 decreased by 30% and 44% respectively. Despite this large perturbation in anthropogenic
28 emissions, the predicted impacts due to the land cover change were fundamentally the same.
29 The range of impact on simulated mean O_3 over the US due to both emissions and dry
30 deposition combined (Simulation 4 – Simulation 1) went from $\Delta\text{O}_3 = [-0.24, +1.45]$ ppb for
31 the 2010 emissions, to $\Delta\text{O}_3 = [-0.34, + 1.35]$ ppb for the 2005 emissions. Likewise, the
32 maximum impact on SOA changed very little, from $\Delta\text{BSOA} = -2.05 \mu\text{g m}^{-3}$ in the 2010

1 simulation, to $\Delta\text{BSOA} = -1.94 \mu\text{g m}^{-3}$ in the 2005 simulation. Nevertheless, simultaneous
2 changes in both anthropogenic and biogenic emissions increase the uncertainty in the exact
3 magnitude of projected changes in secondary pollutants.

4 Many opportunities exist for development and incorporating further complexity. For example,
5 these simulations have not accounted for the temporal dynamics of forests undergoing
6 disturbances from insect attack and disease. In the case of insect infestation, VOC emissions
7 can be enhanced during the attack (Amin et al., 2012), and Berg et al. (2013) found that the
8 spatiotemporal patterns in tree mortality can greatly affect the relative impacts of the attack
9 effect vs. the mortality effect on BVOC emissions. Numerous compounds have been observed
10 to be emitted by trees when under stress (Faiola et al., 2015; Joutsensaari et al., 2015) that
11 GEOS-Chem does not yet represent. Not only have we compared simple “pre-” and “post-”
12 disturbance scenarios ignoring attack effects, but we have not considered forest succession.
13 Extensive mortality caused by insects and disease may be compared to forest fires (Hicke et
14 al., 2012), with growth of surviving trees and understory potentially accelerating (Brown et
15 al., 2010). In such cases, BVOC emissions may not necessarily decrease universally, but the
16 composition of those emissions could change over time. Forest recovery after an outbreak
17 may be possible within decades, as has been predicted in the case of bark beetle outbreak in
18 the western US using a forest vegetation simulator (Pfeifer et al., 2011). Successional
19 dynamics could for example be simulated by an individual-based model (e.g. Shuman et al.
20 (2014)), and used as inputs at various time points in the chemical transport model. We have
21 also assumed that basal BVOC emission factors for the surviving vegetation are the same as
22 pre-disturbance, but experiments have shown for example that monoterpene basal emission
23 can increase significantly after forest thinning (Schade and Goldstein, 2003), which may or
24 may not be a temporary effect.

25 Improvements in the parameterization of O_3 deposition should also be explored. While we
26 find changes in dry deposition velocity to be an important (and in the majority of cases
27 overriding) factor in our simulation of O_3 change, other hypothetical simulations where
28 European crop- and grass-lands were converted to poplar plantations for biomass production
29 found that changes from altered dry deposition velocity were an order of magnitude lower
30 than the change in biogenic emissions (Beltman et al., 2013). Dry deposition rates can depend
31 strongly on the choice of model (Hardacre et al., 2015; Park et al., 2014; Wu et al., 2011),
32 making predictions that depend on this uncertain. Improvements can be expected by more

1 accurate representations of land cover (and subsequent changes) (Hardacre et al., 2015), or by
2 including a more process-based model of deposition that depends on soil moisture and vapour
3 deficit (Büker et al., 2012; Pleim et al., 2001). There is also evidence that a significant
4 fraction of the O₃ uptake observed over forest canopies is actually an unaccounted-for
5 chemical sink (Kurpius and Goldstein, 2003; Rannik et al., 2012; Schade and Goldstein,
6 2003; Wolfe et al., 2011), but changes in this above-canopy chemistry are not captured in our
7 current set of simulations.

8 Likewise, canopy chemistry and stand development post-disturbance will affect the predicted
9 impacts on soil NO_x emissions. The impacts of canopy uptake and canopy chemistry resulting
10 from changes in vegetation density and composition could be explored in more detail with
11 future work using a 1-D forest canopy-chemistry model (e.g. Wolfe 2011; Ashworth et al.
12 2015) for the regions where we project large impacts. We have assumed that the basal
13 emissions from the soil after the disturbance will be the same as those prior to the disturbance,
14 but large scale tree mortality and forest succession have the potential alter soil
15 biogeochemistry (Gao et al., 2015; Norton et al. 2015; Trahan et al., 2015).

16 We anticipate the impacts of tree mortality that are simulated here to be conservative. Future
17 climate change is not included in the NIDR assessment, but is expected to increase the risk of
18 mortality from several pests (Krist et al., 2014). Likewise, insect attack could make certain
19 tree species more sensitive to climate stresses, resulting in mortality despite what might have
20 been otherwise non-lethal insect attack (Anderegg et al., 2015). Predictions over the time
21 scale of years and decades will depend on how the insect/disease disturbances interact with
22 other abiotic environmental disturbances (e.g. drought, extreme heat), but these interactions
23 are rarely fully coupled (Anderegg et al., 2015). Furthermore, tree mortality from many other
24 factors outside of pests and pathogens are not considered (e.g. competition from invasive
25 exotic plants, drought, or other disturbances). As a result, the actual tree loss in the coming
26 decades, and the concomitant impacts on atmospheric chemistry, may be higher than
27 simulated here. We have also ignored any potential feedback between tree mortality and fire
28 incidence or severity, which is not well understood (Bond et al. 2009). Increases in wildfire
29 (and associated emissions) due to climate change have been predicted to have important
30 consequences for ozone air quality (Yue et al. 2015). Finally, our simulations only explored
31 tree mortality across the United States. No similar large-scale projection of mortality risk
32 exists for Canada, despite insect outbreak already being the dominant cause of tree mortality

1 in boreal forests of eastern Canada (Zhang et al. 2014), and severe (although decreasing)
2 mountain pine beetle infestations in western Canada (Buston and Maclachlan, 2014).
3 Increasing insect outbreaks are also a potential threat to forests elsewhere in the world
4 (Lindner et al. 2010). We note that our simulations neglect any potential human intervention
5 in response to these risks.

6

7 **6 Conclusion**

8 Land use and land cover change is expected to be a major driver of global change that remains
9 difficult to constrain. The change in vegetation that we have explored in these simulations
10 represents one of a myriad of changes that are occurring (and are projected to occur) to the
11 Earth's land surface. We anticipate that these GEOS-Chem model developments will enable
12 investigation of a wide range of land cover and land use change impacts (e.g. vegetation
13 succession, deforestation or afforestation, and crop conversions). Properly representing
14 changes in land cover by including accurate and timely updates to chemical transport models
15 will be an important part of simulating global change. By linking all terrestrial biosphere
16 exchange to plant functional type, our GEOS-Chem developments bring the model a step
17 closer to eventual coupling with dynamic vegetation and/or Earth system models.

18 Our results add to the literature demonstrating that changes to vegetation can have significant
19 impacts on local chemistry due to changes in biosphere-atmosphere fluxes of reactive trace
20 species, with consequences for controlling regional air quality. Given the general tightening
21 of air quality standards to improve the health of global populations, understanding how
22 changes in land cover will aid or abet these achievements could become increasingly
23 important.

24

25 **Appendix A: Land Cover Classification System**

26 Table A1 lists the land and plant functional types in the CLM4 land cover description which
27 we use as a base land cover input for our simulations. The table also shows how we have
28 mapped these land cover types to the original Wesely deposition surfaces and to roughness
29 heights for the dry deposition parameterization.

1 Figure A1 schematically lays out how we have defined biomes in accordance with the
2 nomenclature used for soil NO_x emissions based on the CLM4 land and plant functional type
3 coverage.

4

5 **Acknowledgements**

6 This work was supported by NSERC and NSF (AGC-1238109). JAG was partially supported
7 by a NSERC CREATE IACPES postdoctoral fellowship and travel grant.

8

1 **References**

- 2 Alexander, B., Park, R. J., Jacob, D. J., Li, Q. B., Yantosca, R. M., Savarino, J., Lee, C. C. W.
3 and Thiemens, M. H.: Sulfate formation in sea-salt aerosols: Constraints from oxygen
4 isotopes, *J. Geophys. Res.*, 110, D10307, 2005.
- 5 Amin, H., Atkins, P. T., Russo, R. S., Brown, A. W., Sive, B., Hallar, A. G. and Huff Hartz,
6 K. E.: Effect of bark beetle infestation on secondary organic aerosol precursor emissions.,
7 *Environ. Sci. Technol.*, 46(11), 5696–703, doi:10.1021/es204205m, 2012.
- 8 Anderegg, W. R. L., Hicke, J. A., Fisher, R. A., Allen, C. D., Aukema, J., Bentz, B., Hood, S.,
9 Lichstein, J. W., Macalady, A. K., McDowell, N., Pan, Y., Raffa, K., Sala, A., Shaw, J. D.,
10 Stephenson, N. L., Tague, C. and Zeppel, M.: Tree mortality from drought, insects, and their
11 interactions in a changing climate., *New Phytol.*, 208, 674–683, doi:10.1111/nph.13477, 2015.
- 12 Arneth, A., Sitch, S., Bondeau, A., Butterbach-Bahl, K., Foster, P., Gedney, N., de Noblet-
13 Ducoudre, D., Prentice, I.C., Sanderson, M., Thonicke, K., Wania, R., Zaehle, S.: From biota
14 to chemistry and climate: towards a comprehensive description of trace gas exchange between
15 the biosphere and atmosphere, *Biogeosci.*, 7, 212–149, 2010.
- 16 Ashmore, M. R.: Assessing the future global impacts of ozone on vegetation, *Plant, Cell*
17 *Environ.*, 28(8), 949–964, doi:10.1111/j.1365-3040.2005.01341.x, 2005.
- 18 Ashworth, K., Folberth, G., Hewitt, C. N. and Wild, O.: Impacts of near-future cultivation of
19 biofuel feedstocks on atmospheric composition and local air quality, *Atmos. Chem. Phys.*,
20 12(2), 919–939, doi:10.5194/acp-12-919-2012, 2012.
- 21 Ashworth, K., Chung, S. H., Griffin, R. J., Chen, J., Forkel, R., Bryan, A. M., and Steiner, A.
22 L.: FORest Canopy Atmosphere Transfer (FORCAsT) 1.0: a 1-D model of biosphere–
23 atmosphere chemical exchange, *Geosci. Model Dev.*, 8, 3765–3784, doi:10.5194/gmd-8-3765-
24 2015, 2015.
- 25 Beltman, J. B., Hendriks, C., Tum, M. and Schaap, M.: The impact of large scale biomass
26 production on ozone air pollution in Europe, *Atmos. Environ.*, 71, 352–363,
27 doi:10.1016/j.atmosenv.2013.02.019, 2013.
- 28 Berg, A. R., Heald, C. L., Huff Hartz, K. E., Hallar, A. G., Meddens, A. J. H., Hicke, J. A.,
29 Lamarque, J.-F. and Tilmes, S.: The impact of bark beetle infestations on monoterpene

1 emissions and secondary organic aerosol formation in western North America, *Atmos. Chem.*
2 *Phys.*, 13(6), 3149–3161, doi:10.5194/acp-13-3149-2013, 2013.

3 Bey, I., Jacob, D. J., Yantosca, R. M., Logan, J. A., Field, B. D., Fiore, A. M., Li, Q., Liu, H.
4 Y., Mickley, L. J. and Schultz, M. G.: Global modeling of tropospheric chemistry with
5 assimilated meteorology: Model description and evaluation, *J. Geophys. Res.*, 106(D19),
6 23073, doi:10.1029/2001JD000807, 2001.

7 Bonan, G. B.: Forests and climate change: Forcings, feedbacks, and the climate benefits of
8 forests, *Science* (80-.), 320(5882), 1444–1449, 2008.

9 Bond, M. L., Lee D. E., Bradley, C. M. and Hanson, C. T.: Influence of pre-fire tree mortality
10 on fire severity in conifer forests of the San Bernardino Mountains, California, *The Open*
11 *Forest Science Journal*, 2, 41-47, 2009.

12 Brown, M., Black, T. A., Nesic, Z., Foord, V. N., Spittlehouse, D. L., Fredeen, A. L., Grant,
13 N. J., Burton, P. J. and Trofymow, J. A.: Impact of mountain pine beetle on the net ecosystem
14 production of lodgepole pine stands in British Columbia, *Agric. For. Meteorol.*, 150(2), 254–
15 264, doi:10.1016/j.agrformet.2009.11.008, 2010.

16 Büker, P., Morrissey, T., Briolat, A., Falk, R., Simpson, D., Tuovinen, J.-P., Alonso, R.,
17 Barth, S., Baumgarten, M., Grulke, N., Karlsson, P. E., King, J., Lagergren, F., Matyssek, R.,
18 Nunn, A., Ogaya, R., Peñuelas, J., Rhea, L., Schaub, M., Uddling, J., Werner, W. and
19 Emberson, L. D.: DO₃SE modelling of soil moisture to determine ozone flux to forest trees,
20 *Atmos. Chem. Phys.*, 12(12), 5537–5562, doi:10.5194/acp-12-5537-2012, 2012.

21 Buston, K. and Maclachlan L.: 2014 Overview of Forest Health Conditions in Southern
22 British Columbia. Report by the British Columbia Ministry of Forests, Lands, and Natural
23 Resource Operations, Kamloops BC, 2014.

24 Chen, J., Avise, J., Guenther, A., Wiedinmyer, C., Salathe, E., Jackson, R. B. and Lamb, B.:
25 Future land use and land cover influences on regional biogenic emissions and air quality in
26 the United States, *Atmos. Environ.*, 43(36), 5771–5780, doi:10.1016/j.atmosenv.2009.08.015,
27 2009.

28 Dale, V. H., Joyce, L. A., McNulty, S., Neilson, R. P., Ayres, M. P., Flannigan, M. D.,
29 Hanson, P. J., Irland, L. C., Lugo, A. E., Peterson, C. J., Simberloff, D., Swanson, F. J.,
30 Stocks, B. J. and Wotton, M. B.: Climate Change and Forest Disturbances, *Bioscience*, 51(9),
31 723, doi:10.1641/0006-3568(2001)051[0723:CCAFD]2.0.CO;2, 2001.

1 Donahue, N., Robinson, A., Stanier, C., and Pandis, S.: Coupled partitioning, dilution, and
2 chemical aging of semivolatile organics, *Environ. Sci. Technol.*, 40(8), 2635-2643,
3 doi:10.1021/es052297c., 2006.

4 Drewniak, B. A., Snyder, P. K., Steiner, A. L., Twine, T. E. and Wuebbles, D. J.: Simulated
5 changes in biogenic VOC emissions and ozone formation from habitat expansion of *Acer*
6 *Rubrum* (red maple), *Environ. Res. Lett.*, 9(1), 014006, doi:10.1088/1748-9326/9/1/014006,
7 2014.

8 Evans, M. J. and Jacob D.J.: Impact of new laboratory studies of N₂O₅ hydrolysis on global
9 model budgets of tropospheric nitrogen oxides, ozone, and OH, *Geophys. Res. Lett.*, 32(9),
10 L09813, doi:10.1029/2005GL022469, 2005.

11 Evans, M. J. and Sofen, E. D.: Gridded Global Surface Ozone Metrics data (1971-2015) for
12 Atmospheric Chemistry Model Evaluation - version 2.4, *Cent. Environ. Data Anal.*,
13 doi:10.5285/08fbc63d-fa6d-4a7a-b952-5932e3ab0452, 2015.

14 Faiola, C. L., Jobson, B. T. and VanReken, T. M.: Impacts of simulated herbivory on volatile
15 organic compound emission profiles from coniferous plants, *Biogeosciences*, 12(2), 527–547,
16 doi:10.5194/bg-12-527-2015, 2015.

17 Fairlie, T. D., Jacob, D. J. and Park R. J., The impact of transpacific transport of mineral dust
18 in the United States, *Atmos. Environ.*, 1251-1266, 2007.

19 Feddema, J. J., Oleson, K. W., Bonan, G. B., Mearns, L. O., Buja, L. E., Meehl, G. A. and
20 Washington, W. M.: The importance of land-cover change in simulating future climates.,
21 *Science*, 310(5754), 1674–8, doi:10.1126/science.1118160, 2005.

22 Fiore, A. M.: Background ozone over the United States in summer: Origin, trend, and
23 contribution to pollution episodes, *J. Geophys. Res.*, 107(D15), 4275,
24 doi:10.1029/2001JD000982, 2002.

25 Fiore, A. M.: Evaluating the contribution of changes in isoprene emissions to surface ozone
26 trends over the eastern United States, *J. Geophys. Res.*, 110(D12), D12303,
27 doi:10.1029/2004JD005485, 2005.

28 Fisher, J. A., Jacob, D. J., Wang, Q., Bahreini, R., Carouge, C. C., Cubison, M. J., Dibb, J. E.,
29 Diehl, T., Jimenez, J. L., Leibensperger, E. M., Lu, Z., Meinders, M. B. J., Pye, H. O. T.,
30 Quinn, P. K., Sharma, S., Streets, D. G., van Donkelaar, A. and Yantosca, R. M.: Sources,

1 distribution, and acidity of sulfate–ammonium aerosol in the Arctic in winter–spring, *Atmos.*
2 *Environ.*, 45(39), 7301–7318, doi:10.1016/j.atmosenv.2011.08.030, 2011.

3 Fountoukis, C. and Nenes, A.: ISORROPIA II: a computationally efficient thermodynamic
4 equilibrium model for K^+ - Ca^{2+} - Mg^{2+} - NH_4^+ - Na^+ - SO_4^{2-} - NO_3^- - Cl^- - H_2O aerosols,
5 *Atmos. Chem. Phys.*, 7(17), 4639–4659, 2007.

6 Ganzeveld, L.: Impact of Amazonian deforestation on atmospheric chemistry, *Geophys. Res.*
7 *Lett.*, 31(6), L06105, doi:10.1029/2003GL019205, 2004.

8 Ganzeveld, L., Bouwman, L., Stehfest, E., van Vuuren, D. P., Eickhout, B. and Lelieveld, J.:
9 Impact of future land use and land cover changes on atmospheric chemistry-climate
10 interactions, *J. Geophys. Res.*, 115(D23), D23301, doi:10.1029/2010JD014041, 2010.

11 Gao, R., Shi, J., Huang, R., Wang, Z. and Luo, Y.: Effects of pine wilt disease invasion on
12 soil properties and Masson pine forest communities in the Three Gorges reservoir region,
13 China., *Ecol. Evol.*, 5(8), 1702–16, doi:10.1002/ece3.1326, 2015.

14 Guenther, A., Karl, T., Harley, P., Wiedinmyer, C., Palmer, P. I. and Geron, C.: Estimates of
15 global terrestrial isoprene emissions using MEGAN (Model of Emissions of Gases and
16 Aerosols from Nature), *Atmos. Chem. Phys.*, 6, 3181–3210, 2006.

17 Guenther, A. B., Jiang, X., Heald, C. L., Sakulyanontvittaya, T., Duhl, T., Emmons, L. K. and
18 Wang, X.: The Model of Emissions of Gases and Aerosols from Nature version 2.1
19 (MEGAN2.1): an extended and updated framework for modeling biogenic emissions, *Geosci.*
20 *Model Dev.*, 5(6), 1471–1492, doi:10.5194/gmd-5-1471-2012, 2012.

21 Hakami, A., Seinfeld, J. H., Chai, T., Tang, Y., Carmichael, G. R. and Sandu, A.: Adjoint
22 Sensitivity Analysis of Ozone Nonattainment over the Continental United States, *Environ.*
23 *Sci. Technol.*, 40(12), 3855–3864, doi:10.1021/es052135g, 2006.

24 Hardacre, C., Wild, O. and Emberson, L.: An evaluation of ozone dry deposition in global
25 scale chemistry climate models, *Atmos. Chem. Phys.*, 15(11), 6419–6436, doi:10.5194/acp-
26 15-6419-2015, 2015.

27 Hallquist, M., Wenger, J. C., Baltensperger, U., Rudich, Y., Simpson, D., Claeys, M.,
28 Dommen, J., Donahue, N. M., George, C., Goldstein, A. H., Hamilton, J. F., Herrmann, H.,
29 Hoffmann, T., Iinuma, Y., Jang, M., Jenkin, M. E., Jiminez, J. L., Kiendler-Scharr, A.,
30 Maenhautt W., McFiggans, G., Mentel, Th. F., Monod, A., Prevot, A. S. H., Seinfeld, J. H.,

1 Surratt, J. D., Szmigielski, R., and Wildt., J.: The formation, properties and impact of
2 secondary organic aerosol: current and emerging issues, *Atmos. Chem. Phys.*, 9, 5155-5236,
3 doi:10.5194/acp-9-5155-2009, 2009.

4 Hardacre, C. J., Palmer, P. I., Baumanns, K., Rounsevell, M. and Murray-Rust, D.:
5 Probabilistic estimation of future emissions of isoprene and surface oxidant chemistry
6 associated with land-use change in response to growing food needs, *Atmos. Chem. Phys.*,
7 13(11), 5451–5472, doi:10.5194/acp-13-5451-2013, 2013.

8 Heald, C. L. and Spracklen, D. V: Land Use Change Impacts on Air Quality and Climate.,
9 *Chem. Rev.*, 115(10), 4476–4496, doi:10.1021/cr500446g, 2015.

10 Heald, C. L., Henze, D. K., Horowitz, L. W., Feddema, J., Lamarque, J.-F., Guenther, A.,
11 Hess, P. G., Vitt, F., Seinfeld, J. H., Goldstein, A. H. and Fung, I.: Predicted change in global
12 secondary organic aerosol concentrations in response to future climate, emissions, and land
13 use change, *J. Geophys. Res. Atmos.*, 113, D05211, doi:10.1029/2007JD009092, 2008.

14 Hicke, J. A., Allen, C. D., Desai, A. R., Dietze, M. C., Hall, R. J., Ted Hogg, E. H., Kashian,
15 D. M., Moore, D., Raffa, K. F., Sturrock, R. N. and Vogelmann, J.: Effects of biotic
16 disturbances on forest carbon cycling in the United States and Canada, *Glob. Chang. Biol.*,
17 18(1), 7–34, doi:10.1111/j.1365-2486.2011.02543.x, 2012.

18 Horowitz, L. W., Walters, S., Mauzerall, D. L., Emmons, L. K., Rasch, P. J., Grainier, C., Tie,
19 X., Lamarque, J. -F., Schultz, M. G., Tyndall, G. S., Orlando, J. J. and Brasseur, G. P.: A
20 global simulation of tropospheric ozone and related tracers: Description and evaluation of
21 MOZART, version 2, *J. Geophys. Res. Atmos.*, 108(D24), doi:10.1029/2002JD002853, 2003.

22 Hudman, R. C., Moore, N. E., Mebust, A. K., Martin, R. V, Russell, A. R., Valin, L. C. and
23 Cohen, R. C.: Steps towards a mechanistic model of global soil nitric oxide emissions:
24 implementation and space based-constraints, *Atmos. Chem. Phys.*, 12(16), 7779–7795,
25 doi:10.5194/acp-12-7779-2012, 2012.

26 Joutsensaari, J., Yli-Pirilä, P., Korhonen, H., Arola, A., Blande, J. D., Heijari, J.,
27 Kivimäenpää, M., Mikkonen, S., Hao, L., Miettinen, P., Lyytikäinen-Saarenmaa, P., Faiola,
28 C. L., Laaksonen, A. and Holopainen, J. K.: Biotic stress accelerates formation of climate-
29 relevant aerosols in boreal forests, *Atmos. Chem. Phys. Discuss.*, 15(7), 10853–10898,
30 doi:10.5194/acpd-15-10853-2015, 2015.

1 Kim, H.-K., Woo, J.-H., Park, R. S., Song, C. H., Kim, J.-H., Ban, S.-J. and Park, J.-H.:
2 Impacts of different plant functional types on ambient ozone predictions in the Seoul
3 Metropolitan Areas (SMAs), Korea, *Atmos. Chem. Phys.*, 14(14), 7461–7484,
4 doi:10.5194/acp-14-7461-2014, 2014.

5 Krist, F. J. J., Ellenwood, J. R., Woods, M. E., McMahan, A. J., Cowardin, J. P., Ryerson, D.
6 E., Saplo, F. J., Zwelfler, M. O. and Romero, S. A.: National Insect and Disease Forest Risk
7 Assessment 2013-2027, Fort Collins, CO. [online] Available from:
8 <http://www.fs.fed.us/foresthealth/technology> (last access: 23 October 2015), 2014.

9 Kuhns, H., Knipping, E. M. and Vukovich, J. M.: Development of a United States-Mexico
10 Emissions Inventory for the Big Bend Regional Aerosol and Visibility Observational
11 (BRAVO) Study., *J. Air Waste Manag. Assoc.*, 55(5), 677–92, 2005.

12 Kurpius, M. R. and Goldstein, A. H.: Gas-phase chemistry dominates O₃ loss to a forest,
13 implying a source of aerosols and hydroxyl radicals to the atmosphere, *Geophys. Res. Lett.*,
14 30(7), 1371, doi:10.1029/2002GL016785, 2003.

15 Laothawornkitkul, J., Taylor, J. E., Paul, N. D., Hewitt, C. N.: Biogenic volatile organic
16 compounds in the Earth System, *New Phytol.*, 183(1), 27-51, 2009.

17 Lawrence, D. M., Oleson, K. W., Flanner, M. G., Thornton, P. E., Swenson, S. C., Lawrence,
18 P. J., Zeng, X., Yang, Z.-L., Levis, S., Sakaguchi, K., Bonan, G. B. and Slater, A. G.:
19 Parameterization improvements and functional and structural advances in Version 4 of the
20 Community Land Model, *J. Adv. Model. Earth Syst.*, 3(3), M03001,
21 doi:10.1029/2011MS000045, 2011.

22 Li, M., Wang, Y. and Ju, W.: Effects of a remotely sensed land cover dataset with high spatial
23 resolution on the simulation of secondary air pollutants over china using the nested-grid
24 GEOS-chem chemical transport model, *Adv. Atmos. Sci.*, 31(1), 179–187,
25 doi:10.1007/s00376-013-2290-1, 2013.

26 Lindner, M., Maroschek, M., Netherer, S., Kremer, A., Barbati, A., Garcia-Gonzalo, J., Seidl,
27 R., Delzon, S., Corona, P., Kolstrom, M., Lexer, M., Marchetti, M.: Climate change impacts,
28 adaptive capacity, and vulnerability of European forest ecosystems, *Forest Ecol. Manag.*, 259,
29 698-709, 2010.

30 MacKenzie, A. R., Langford, B., Pugh, T. A. M., Robinson, N., Misztal, P. K., Heard, D. E.,
31 Lee, J. D., Lewis, A. C., Jones, C. E., Hopkins, J. R., Phillips, G., Monks, P. S., Karunaharan,

1 A., Hornsby, K. E., Nicolas-Perea, V., Coe, H., Gabey, A. M., Gallagher, M. W., Whalley, L.
2 K., Edwards, P. M., Evans, M. J., Stone, D., Ingham, T., Commane, R., Furneaux, K. L.,
3 McQuaid, J. B., Nemitz, E., Seng, Y., Fowler, D., Pyle, J. A. and Hewitt, C. N.: The
4 atmospheric chemistry of trace gases and particulate matter emitted by different land uses in
5 Borneo, *Philos. Trans. R. Soc. B Biol. Sci.*, 366(1582), 3177–3195, 2011.

6 Mao, J., Fan, S., Jacob, D. J. and Travis, K. R.: Radical loss in the atmosphere from Cu-Fe
7 redox coupling in aerosols, *Atmos. Chem. Phys.*, 13(2), 509–519, doi:10.5194/acp-13-509-
8 2013, 2013a.

9 Mao, J., Paulot, F., Jacob, D. J., Cohen, R. C., Crouse, J. D., Wennberg, P. O., Keller, C. A.,
10 Hudman, R. C., Barkley, M. P. and Horowitz, L. W.: Ozone and organic nitrates over the
11 eastern United States: Sensitivity to isoprene chemistry. *J. Geophys. Res. Atmos.*, 118,
12 11256-11268, doi:10.1002/jgrd.50817, 2013.

13 MEA: Ecosystems and human well-being (Millennium Ecosystem Assessment, World Health
14 Organization). [online] Available from: <http://www.who.int/globalchange/ecosystems> (last
15 access: 23 October 2015), 2005.

16 Monson, R. K. and Holland, E. A.: Biospheric trace gas fluxes and their control over
17 tropospheric chemistry, *Annu. Rev. Ecol. Syst.*, 32, 547–576, 2001.

18 Mellouki, A., Wallington, T. J., Chen, J.: Atmospheric chemistry of oxygenated volatile
19 organic compounds: Impacts on air quality and climate, *Chem. Rev.*, 115(10), 3984-4014,
20 doi: 10.1021/cr500549n, 2015.

21 Mu, M., Randerson, J. T., van der Werf, G. R., Giglio, L., Kasibhatla, P., Morton, D., Collatz,
22 G. J., DeFries, R. S., Hyer, E. J., Prins, E. M., Griffith, D. W. T., Wunch, D., Toon, G. C.,
23 Sherlock, V. and Wennberg, P. O.: Daily and 3-hourly variability in global fire emissions and
24 consequences for atmospheric model predictions of carbon monoxide, *J. Geophys. Res.*
25 *Atmos.*, 116, D24303, doi:10.1029/2011JD016245, 2011.

26 Murray, L. T., Jacob, D. J., Logan, J. A., Hudman, R. C. and Koshak, W. J.: Optimized
27 regional and interannual variability of lightning in a global chemical transport model
28 constrained by LIS/OTD satellite data, *J. Geophys. Res. Atmos.*, 117, D20307,
29 doi:10.1029/2012JD017934, 2012.

30 Myneni, R. B., Yang, W., Nemani, R. R., Huete, A. R., Dickinson, R. E., Knyazikhin, Y.,
31 Didan, K., Fu, R., Negrón Juárez, R. I., Saatchi, S. S., Hashimoto, H., Ichii, K., Shabanov, N.

1 V, Tan, B., Ratana, P., Privette, J. L., Morissette, J. T., Vermote, E. F., Roy, D. P., Wolfe, R.
2 E., Friedl, M. A., Running, S. W., Votava, P., El-Saleous, N., Devadiga, S., Su, Y. and
3 Salomonson, V. V: Large seasonal swings in leaf area of Amazon rainforests., *Proc. Natl.*
4 *Acad. Sci. U. S. A.*, 104(12), 4820–3, doi:10.1073/pnas.0611338104, 2007.

5 Norton, U., Ewers, B. E., Borkhuu, B., Brown, N. R. and Pendall, E.: Soil Nitrogen Five
6 Years after Bark Beetle Infestation in Lodgepole Pine Forests, *SOIL Sci. Soc. Am. J.*, 79(1),
7 282–293, doi:10.2134/csa2015-60-2-5, 2015.

8 Odum, J. R., Hoffmann, T., Bowman, F., Collins, D., Flagan, R. C., and Seinfeld, J. H.:
9 Gas/particle partitioning and secondary organic aerosol yields, *Environ. Sci. Technol.*, 30,
10 2580–2585, 1996

11 Park, R. J., Jacob, D. J., Chin, M. and Martin, R. V.: Sources of carbonaceous aerosols over
12 the United States and implications for natural visibility, *J. Geophys. Res.*, 108(D12), 4355,
13 doi:10.1029/2002JD003190, 2003.

14 Park, R. J., Jacob, D. J., Field, B. D. and Yantosca, R. M.: Natural and transboundary
15 pollution influences on sulfate-nitrate-ammonium aerosols in the United States: Implications
16 for policy, *J. Geophys. Res.*, 109(D15), D15204, doi:10.1029/2003JD004473, 2004.

17 Park, R. J., Hong, S. K., Kwon, H.-A., Kim, S., Guenther, A., Woo, J.-H. and Loughner, C.
18 P.: An evaluation of ozone dry deposition simulations in East Asia, *Atmos. Chem. Phys.*,
19 14(15), 7929–7940, doi:10.5194/acp-14-7929-2014, 2014.

20 Paulot, F., Crounse, J. D., Kjaergaard, H. G., Kroll, J. H., Seinfeld, J. H. and Wennberg, P. O.:
21 Isoprene photooxidation: new insights into the production of acids and organic nitrates,
22 *Atmos. Chem. Phys.*, 9(4), 1479–1501, 2009a.

23 Paulot, F., Crounse, J. D., Kjaergaard, H. G., Kürten, A., St Clair, J. M., Seinfeld, J. H. and
24 Wennberg, P. O.: Unexpected epoxide formation in the gas-phase photooxidation of
25 isoprene., *Science*, 325(5941), 730–3, doi:10.1126/science.1172910, 2009b.

26 Pfeifer, E. M., Hicke, J. A. and Meddens, A. J. H.: Observations and modeling of
27 aboveground tree carbon stocks and fluxes following a bark beetle outbreak in the western
28 United States, *Glob. Chang. Biol.*, 17(1), 339–350, doi:10.1111/j.1365-2486.2010.02226.x,
29 2011.

1 Pielke, R. A., Pitman, A., Niyogi, D., Mahmood, R., McAlpine, C., Hossain, F., Goldewijk,
2 K. K., Nair, U., Betts, R., Fall, S., Reichstein, M., Kabat, P. and de Noblet, N.: Land use/land
3 cover changes and climate: modeling analysis and observational evidence, *Wiley Interdiscip.*
4 *Rev. Clim. Chang.*, 2(6), 828–850, doi:10.1002/wcc.144, 2011.

5 Pleim, J. E., Xiu, A., Finkelstein, P. L. and Otte, T. L.: A Coupled Land-Surface and Dry
6 Deposition Model and Comparison to Field Measurements of Surface Heat, Moisture, and
7 Ozone Fluxes, *Water, Air Soil Pollut. Focus*, 1(5-6), 243–252,
8 doi:10.1023/A:1013123725860, 2001.

9 Porter, W. C., Barsanti, K. C., Baughman, E. C. and Rosenstiel, T. N.: Considering the air
10 quality impacts of bioenergy crop production: A case study involving *arundo donax*, *Environ.*
11 *Sci. Tech.*, 46(17), 9777-9784, 2012.

12 Purves, D. W., Caspersen, J. P., Moorcroft, P. R., Hurtt, G. C. and Pacala, S. W.: Human-
13 induced changes in US biogenic volatile organic compound emissions: evidence from long-
14 term forest inventory data, *Glob. Chang. Biol.*, 10(10), 1737–1755, doi:10.1111/j.1365-
15 2486.2004.00844.x, 2004.

16 Pye, H. O. T., Chan, A. W. H., Barkley, M. P. and Seinfeld, J. H.: Global modeling of organic
17 aerosol: the importance of reactive nitrogen (NO_x and NO₃), *Atmos. Chem. Phys.*, 10(22),
18 11261–11276, doi:10.5194/acp-10-11261-2010, 2010.

19 Rannik, Ü., Altimir, N., Mammarella, I., Bäck, J., Rinne, J., Ruuskanen, T. M., Hari, P.,
20 Vesala, T. and Kulmala, M.: Ozone deposition into a boreal forest over a decade of
21 observations: evaluating deposition partitioning and driving variables, *Atmos. Chem. Phys.*,
22 12(24), 12165–12182, doi:10.5194/acp-12-12165-2012, 2012.

23 Sakulyanontvittaya, T., Duhl, T., Wiedinmyer, C., Helmig, D., Matsunaga, S., Potosnak, M.,
24 Milford, J. and Guenther, A.: Monoterpene and Sesquiterpene Emission Estimates for the
25 United States, *Environ. Sci. Technol.*, 42(5), 1623–1629, doi:10.1021/es702274e, 2008.

26 Schade, G. W. and Goldstein, A.: Increase of monoterpene emissions from a pine plantation
27 as a result of mechanical disturbances, *Geophys. Res. Lett.*, 30(7), 1380,
28 doi:10.1029/2002GL016138, 2003.

29 Shuman, J. K., Shugart, H. H. and Krankina, O. N.: Testing individual-based models of forest
30 dynamics: Issues and an example from the boreal forests of Russia, *Ecol. Modell.*, 293, 102–
31 110, doi:10.1016/j.ecolmodel.2013.10.028, 2014.

1 Smith, P., Gregory, P. J., van Vuuren, D., Obersteiner, M., Havlik, P., Rounsevell, M.,
2 Woods, J., Stehfest, E. and Bellarby, J.: Competition for land., *Philos. Trans. R. Soc. Lond. B.*
3 *Biol. Sci.*, 365(1554), 2941–57, doi:10.1098/rstb.2010.0127, 2010.

4 Smith, W. B., Vissage, J. S., Darr, D. R. and Sheffield, R. M.: Forest resources of the United
5 States, 1997, St. Paul, MN. [online] Available from:
6 http://www.nrs.fs.fed.us/pubs/gtr/gtr_nc219.pdf (last access: 23 October 2015), 2001.

7 Steinkamp, J. and Lawrence, M. G.: Improvement and evaluation of simulated global
8 biogenic soil NO emissions in an AC-GCM, *Atmos. Chem. Phys.*, 11(12), 6063–6082,
9 doi:10.5194/acp-11-6063-2011, 2011.

10 Taylor, G. E., Johnson, D. W. and Andersen, C. P.: Air Pollution and Forest Ecosystems: A
11 Regional to Global Perspective, *Ecol. Appl.*, 4(4), 662, doi:10.2307/1941999, 1994.

12 Trahan, N. A., Dynes, E. L., Pugh, E., Moore, D. J. P. and Monson, R. K.: Changes in soil
13 biogeochemistry following disturbance by girdling and mountain pine beetles in subalpine
14 forests., *Oecologia*, 177(4), 981–95, doi:10.1007/s00442-015-3227-4, 2015.

15 Unger, N.: Human land-use-driven reduction of forest volatiles cools global climate, *Nature*
16 *Clim. Change*, 4, 907-910, 2014.

17 van Donkelaar, A., Martin, R. V., Leaitch, W. R., Macdonald, A. M., Walker, T. W., Streets,
18 D. G., Zhang, Q., Dunlea, E. J., Jimenez, J. L., Dibb, J. E., Huey, L. G., Weber, R. and
19 Andreae, M. O.: Analysis of aircraft and satellite measurements from the Intercontinental
20 Chemical Transport Experiment (INTEX-B) to quantify long-range transport of East Asian
21 sulfur to Canada, *Atmos. Chem. Phys.*, 8(11), 2999–3014, doi:10.5194/acp-8-2999-2008,
22 2008.

23 Van Vuuren, D. P., Edmonds, J., Kainuma, M., Riahi, K., Thomson, A., Hibbard, K., Hurtt,
24 G. C., Kram, T., Krey, V., Lamarque, J.-F., Masui, T., Meinshausen, M., Nakicenovic, N.,
25 Smith, S. J. and Rose, S. K.: The representative concentration pathways: an overview, *Clim.*
26 *Change*, 109(1-2), 5–31, doi:10.1007/s10584-011-0148-z, 2011.

27 Wang, Y. H., Jacob, D. J. and Logan, J. A.: Global simulation of tropospheric O₃-NO_x-
28 hydrocarbon chemistry 1. Model formulation, *J. Geophys. Res.*, 103(D9), 10713–10725,
29 doi:10.1029/98JD00158, 1998.

1 Wesely, M. L.: Parameterization of surface resistances to gaseous dry deposition in regional-
2 scale numerical models, *Atmos. Environ.*, 23(6), 1293–1304, doi:10.1016/0004-6981(89),
3 90153-4, 1989.

4 Wiedinmyer, C., Tie, X., Guenther, A., Neilson, R. and Granier, C.: Future Changes in
5 Biogenic Isoprene Emissions: How Might They Affect Regional and Global Atmospheric
6 Chemistry?, *Earth Interact.*, 10, 1–19, doi: <http://dx.doi.org/10.1175/EI174.1>, 2006.

7 Wolfe, G. M., Thornton, J. A., McKay, M. and Goldstein, A. H.: Forest-atmosphere exchange
8 of ozone: sensitivity to very reactive biogenic VOC emissions and implications for in-canopy
9 photochemistry, *Atmos. Chem. Phys.*, 11(15), 7875–7891, doi:10.5194/acp-11-7875-2011,
10 2011.

11 Wu, S., Mickley, L. J., Jacob, D. J., Rind, D. and Streets, D. G.: Effects of 2000–2050
12 changes in climate and emissions on global tropospheric ozone and the policy-relevant
13 background surface ozone in the United States, *J. Geophys. Res.*, 113(D18), D18312,
14 doi:10.1029/2007JD009639, 2008.

15 Wu, S., Mickley, L. J., Kaplan, J. O. and Jacob, D. J.: Impacts of changes in land use and land
16 cover on atmospheric chemistry and air quality over the 21st century, *Atmos. Chem. Phys.*,
17 12(3), 1597–1609, doi:10.5194/acp-12-1597-2012, 2012.

18 Wu, Z., Wang, X., Chen, F., Turnipseed, A. A., Guenther, A. B., Niyogi, D., Charusombat,
19 U., Xia, B., William Munger, J. and Alapaty, K.: Evaluating the calculated dry deposition
20 velocities of reactive nitrogen oxides and ozone from two community models over a
21 temperate deciduous forest, *Atmos. Environ.*, 45(16), 2663–2674, 2011.

22 Yue, X., Micley, L. J., Logan, J. A., Hudman, R. C., Martin, M. V. and Yantosca, R. M.:
23 Impact of 2050 climate change on North American wildfire: consequences for ozone air
24 quality, *Atmos. Chem. Phys.*, 15, 10033-10055, doi:105194/acp-15-10033-2015, 2015.

25 Zare, A., Christensen, J. H., Irannejad, P. and Brandt, J.: Evaluation of two isoprene emission
26 models for use in a long-range air pollution model, *Atmos. Chem. Phys.*, 12(16), 7399–7412,
27 doi:10.5194/acp-12-7399-2012, 2012.

28 Zare, A., Christensen, J. H., Gross, A., Irannejad, P., Glasius, M. and Brandt, J.: Quantifying
29 the contributions of natural emissions to ozone and total fine PM concentrations in the
30 Northern Hemisphere, *Atmos. Chem. Phys.*, 14(6), 2735–2756, doi:10.5194/acp-14-2735-
31 2014, 2014.

1 Zhang, L. M., Gong, S. L., Padro, J. and Barrie, L.: A size-segregated particle dry deposition
2 scheme for an atmospheric aerosol module, *Atmos. Environ.*, 35(3), 549-560,
3 doi:10.1016/s1352-2310(00)00326-5, 2001.

4 Zhang, X., Lei, Y., Ma, Z., Kneeshaw, D. and Peng, C.: Insect-induced tree mortality of
5 boreal forests in eastern Canada under a changing climate, *Ecol. Evol.*, 4(12), 2384-2394,
6 doi:10.1002/ece3.988, 2014.

7

1 Table 1:

Simulation	Description
1	Base land cover simulation (no tree mortality)
2	Tree mortality-driven BVOC emissions (soil NO _x and dry deposition using base land cover)
3	Tree mortality-driven BVOC and soil NO _x emissions (dry deposition using base land cover)
4	Tree mortality-driven emissions and dry deposition.

2

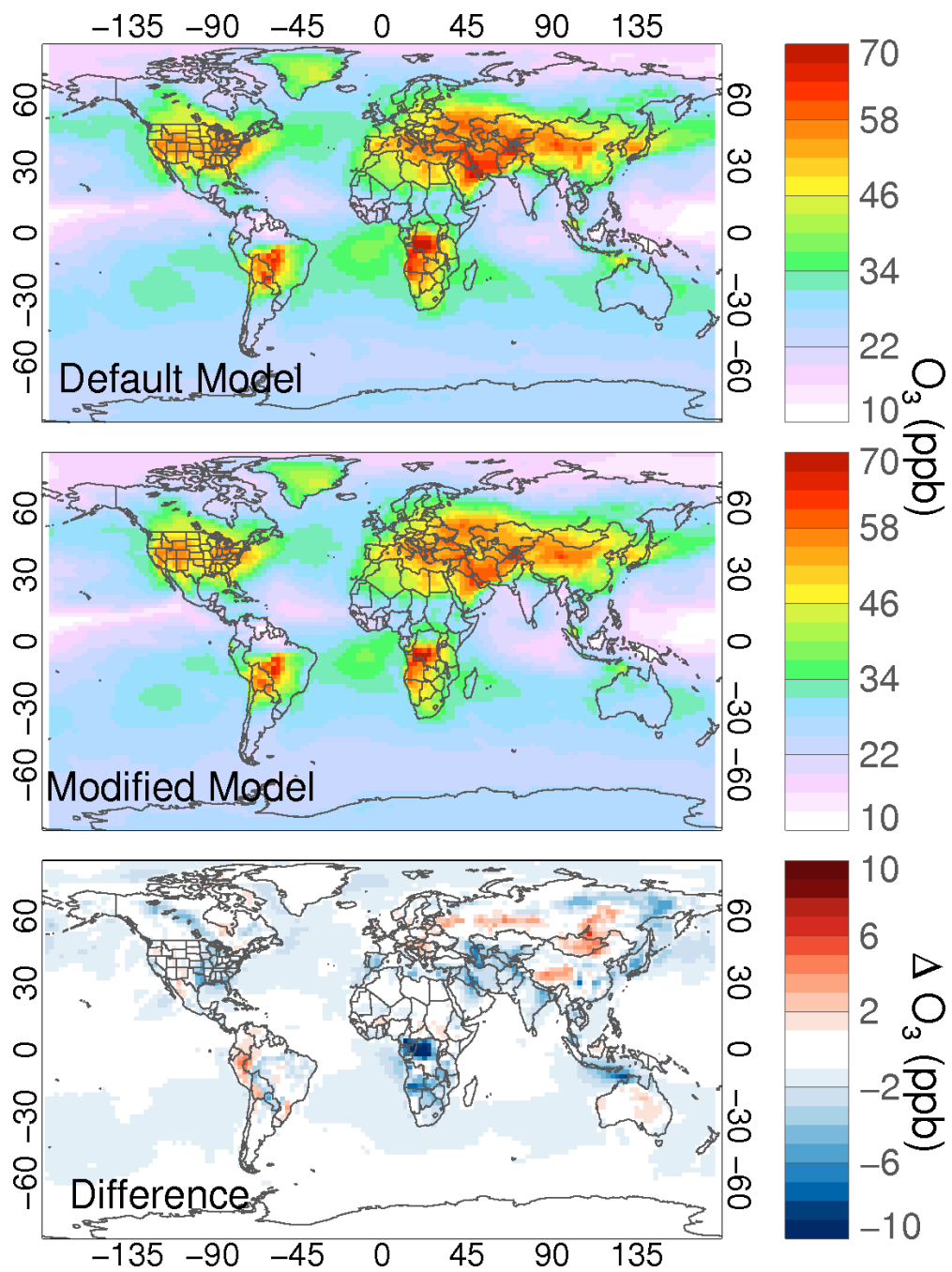
3

1 Table A1: Mapping of CLM-input land types used in the modified version of GEOS-Chem to
 2 the Wesely deposition surfaces for deposition, and the associated roughness (Z_0) heights for
 3 each.

4

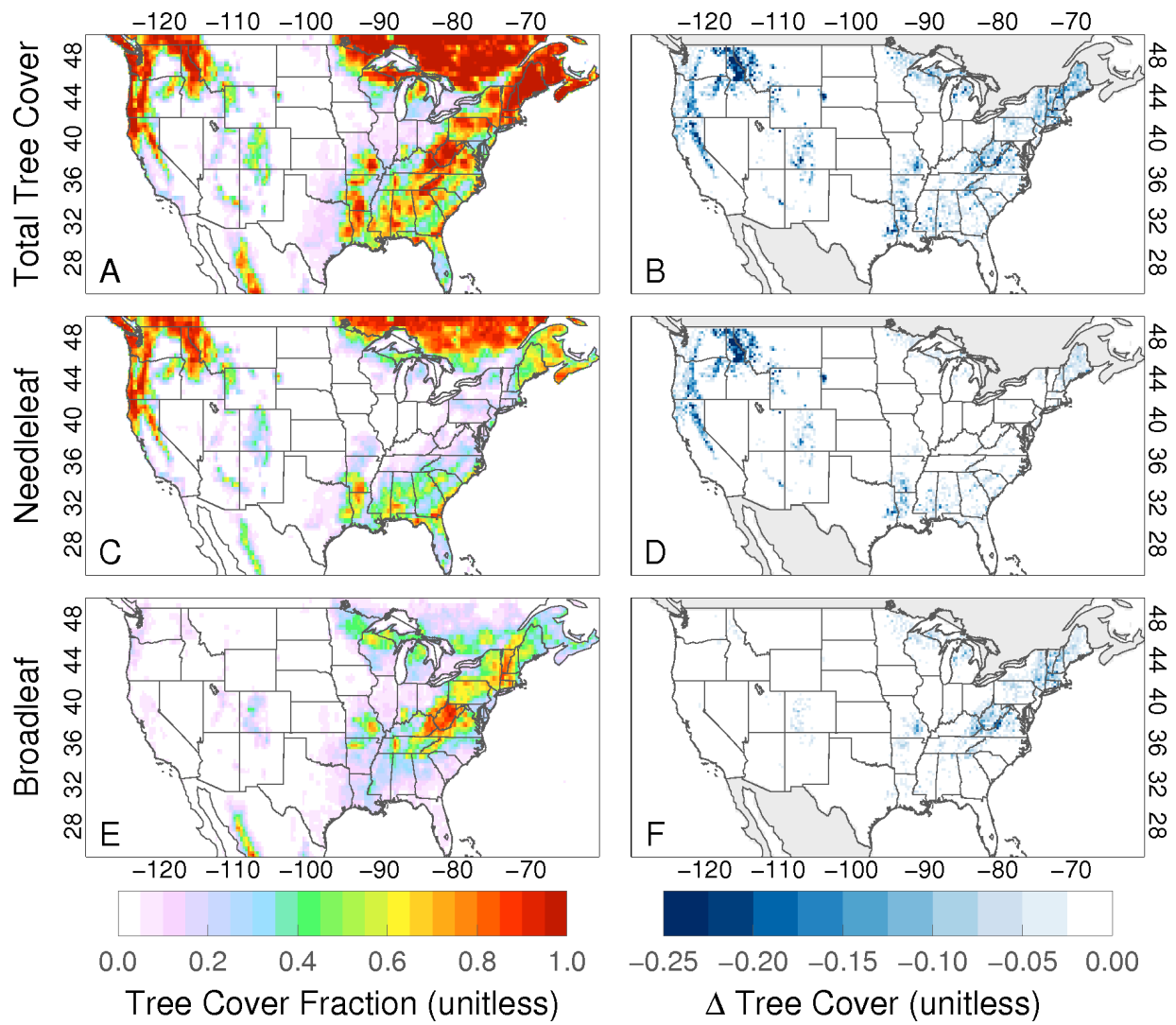
Land Type	Wesely Surface	Z_0 (m)
Lake/Ocean	Water	0.001
Bare Ground	Desert	0.001
NET Temp	Coniferous Forest	1
NET Boreal	Coniferous Forest	1
NDT Boreal	Coniferous Forest	1
BET Trop	Amazon Rainforest	1
BET Temp	Deciduous Forest	1
BDT Trop	Deciduous Forest	1
BDT Temp	Deciduous Forest	1
BDT Boreal	Deciduous Forest	1
BES Temp	Shrub/Grassland	0.01
BDS Temp	Shrub/Grassland	0.01
BDS Boreal	Shrub/Grassland	0.01
C3 Arctic GR	Tundra	0.002
C3 Other GR	Shrub/Grassland	0.01
C4 GR	Shrub/Grassland	0.01
Crop	Agricultural	0.1
Glacier	Snow/Ice	0.0001
Urban	Urban	2.5
Wetland	Wetland	0.05

5



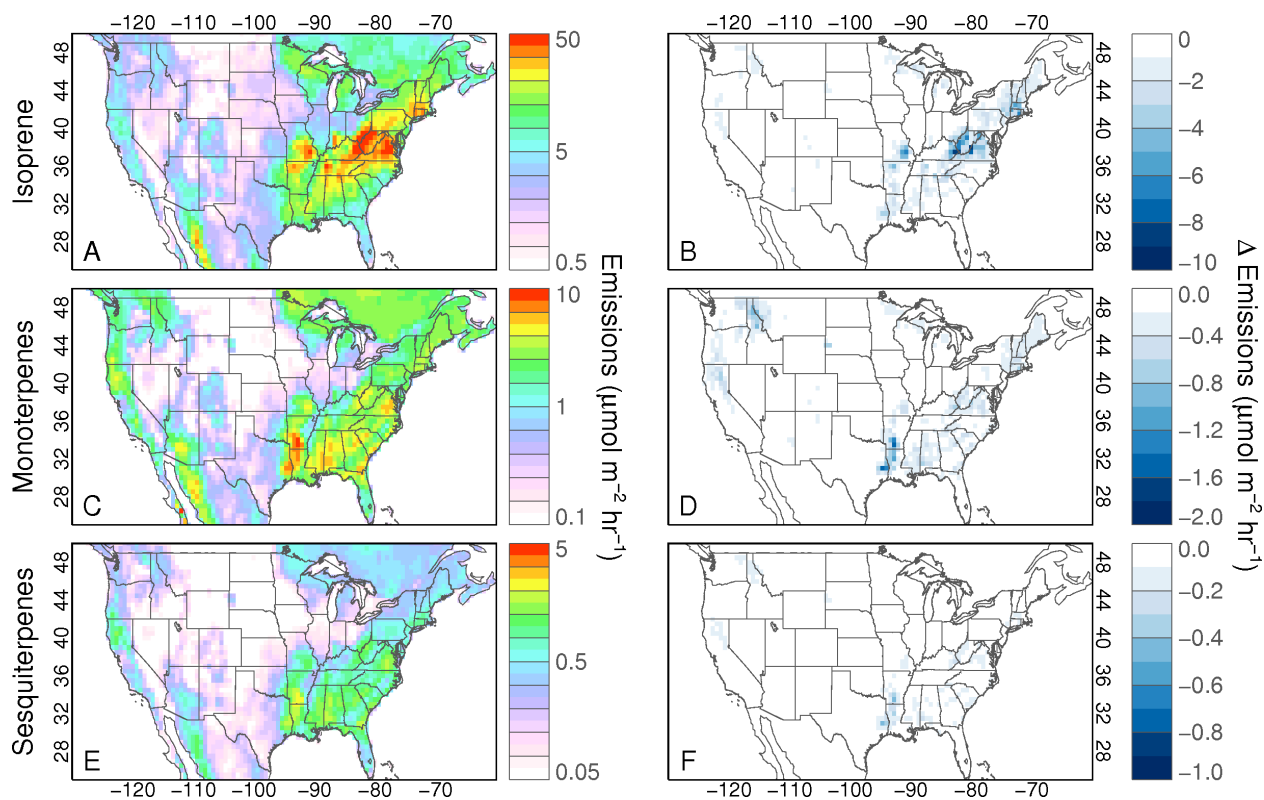
1
2
3
4
5
6

Figure 1. Simulated global surface O_3 concentrations for August 2010 in the (top) default, and (middle) modified GEOS-Chem configuration. (Bottom) Difference between the modified and default simulations.



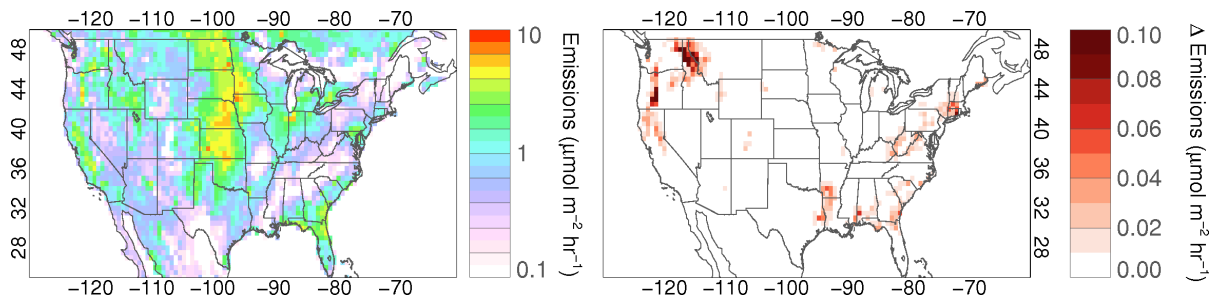
1
2
3
4
5
6
7

Figure 2. Fraction of grid box covered by trees in present day (left), and the loss in tree cover due to predicted mortality from 2013-2027 based on the National Insect and Disease Risk Map (right). (A,B) Total tree cover; (C,D) Needleleaf tree cover only; (E,F) Broadleaf tree cover only.



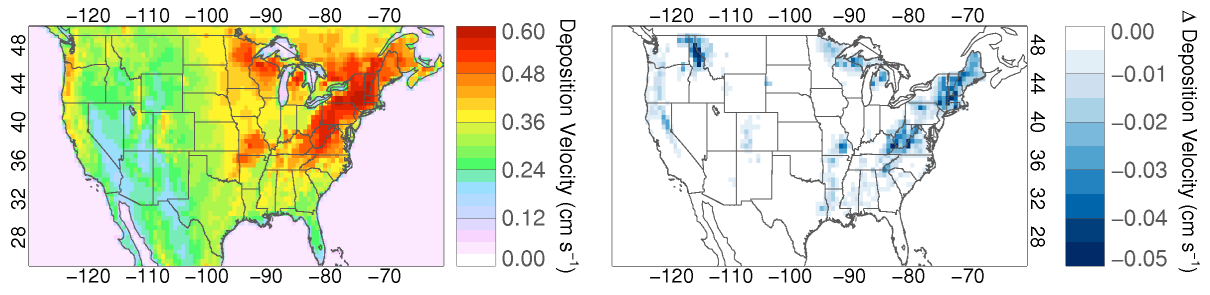
1
2
3
4
5
6

Figure 3. Mean JJA (June-July-August) biogenic VOC emissions in the base scenario (left), and the change in emissions resulting from predicted tree mortality (right). (A,B) Isoprene emissions; (C,D): Total monoterpene emissions; (E,F); Total sesquiterpene emissions.



1
2
3
4
5

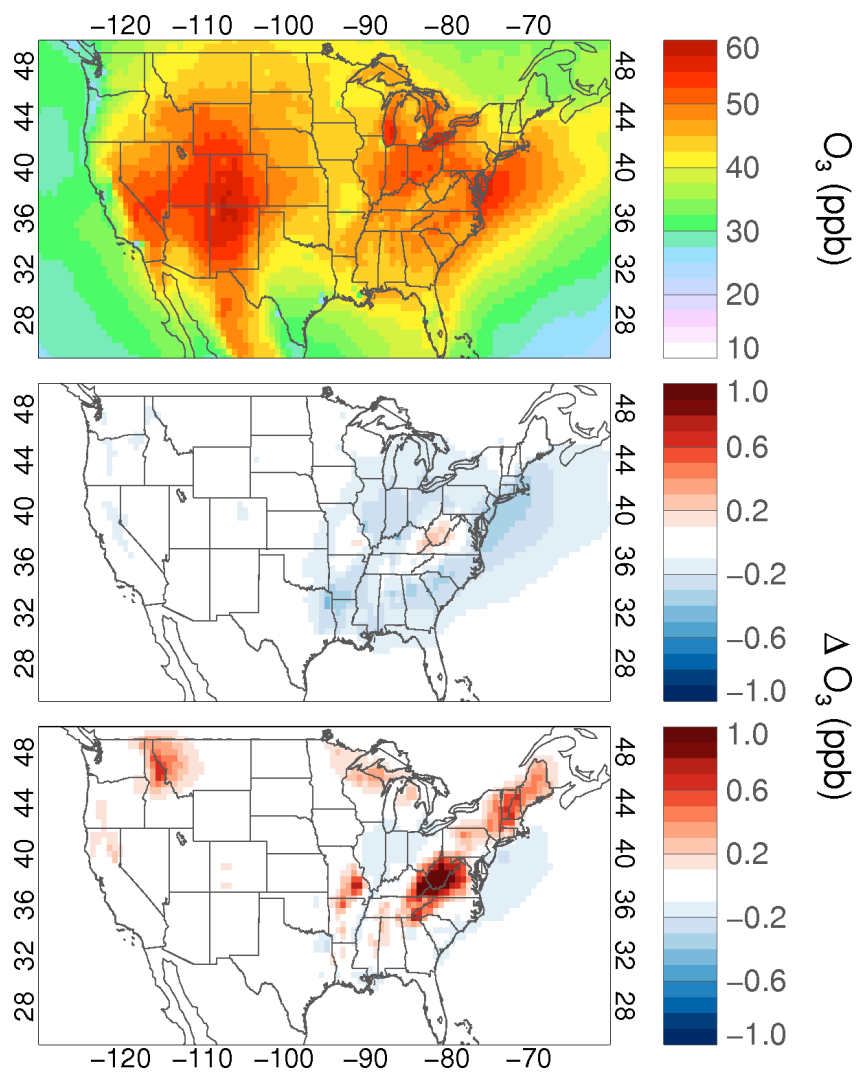
Figure 4. Mean JJA soil NOx emissions in the base scenario for (left), and the change in emissions resulting from predicted tree mortality (right).



1

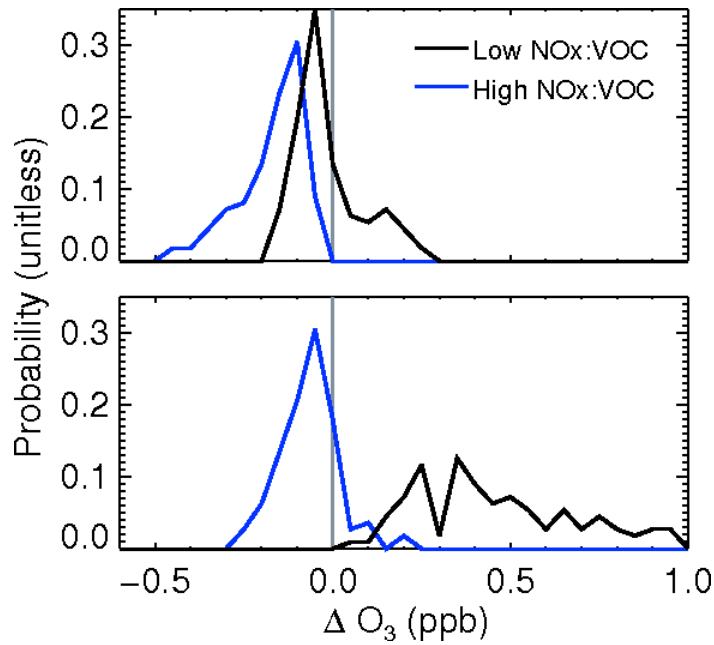
2 Figure 5. Mean JJA O₃ deposition velocity in the base scenario (left), and the change in
3 deposition velocity resulting from predicted tree mortality (right).

4



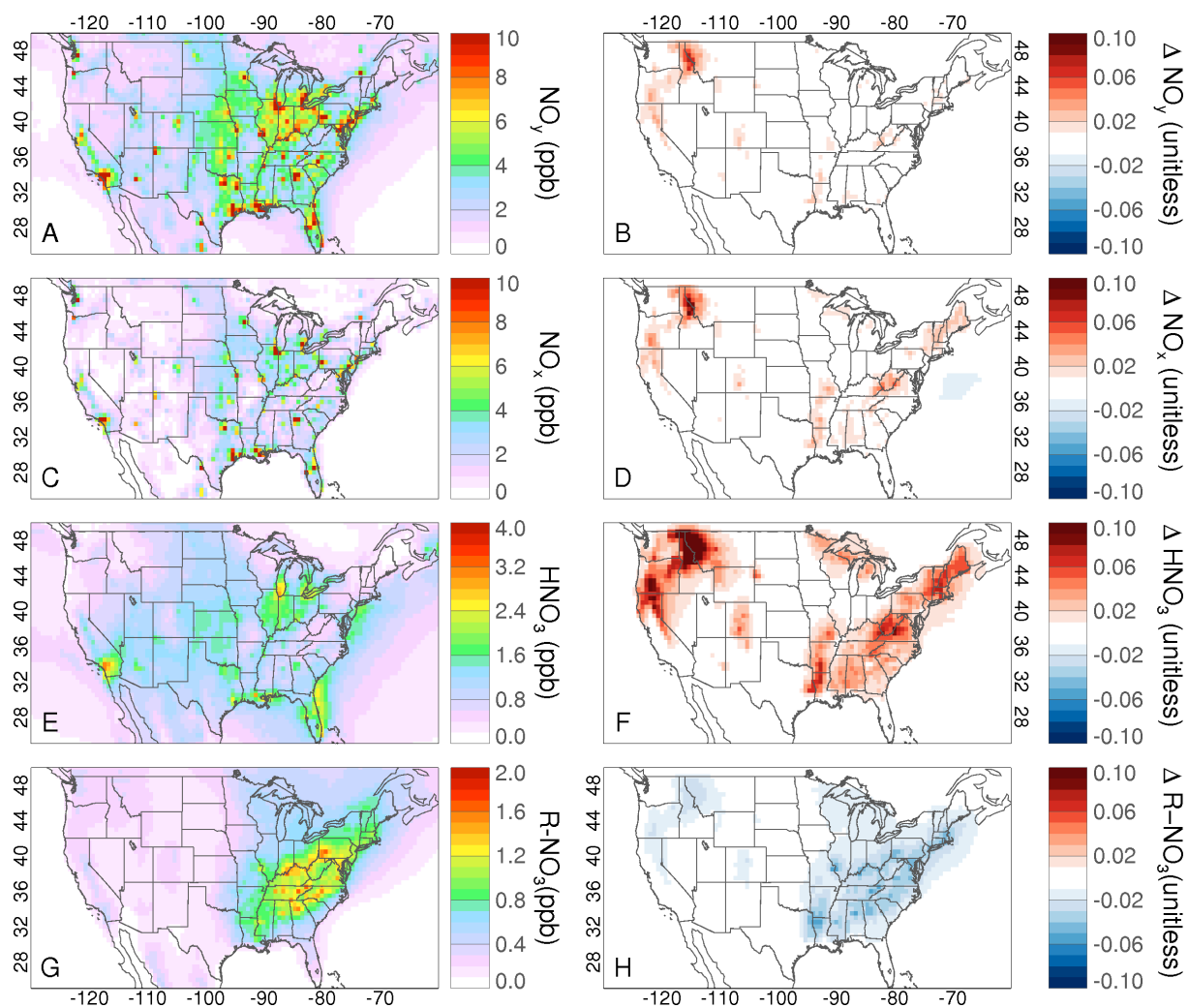
1
2
3
4
5
6
7
8

Figure 6. Top: mean JJA surface O_3 concentrations in the base simulation (Simulation 1). Middle: the change in O_3 concentrations resulting from mortality-driven changes in emissions only (Simulation 3 – Simulation 1). Bottom: the change in O_3 concentrations resulting from mortality driven changes in emissions and deposition velocity together (Simulation 4 – Simulation 1).



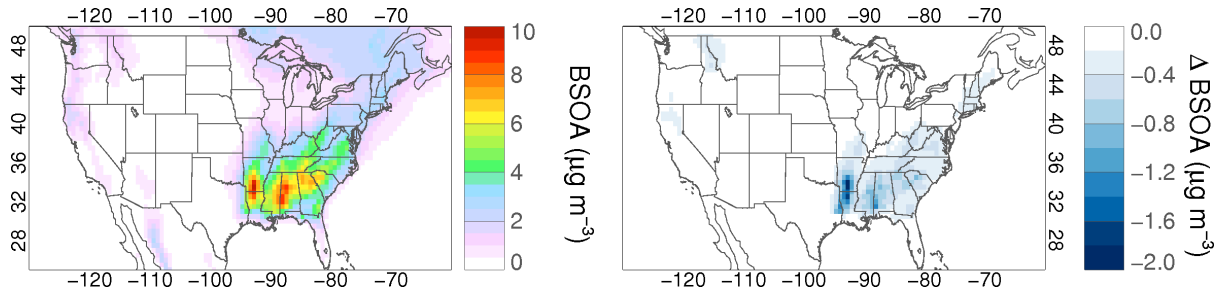
1
2
3
4
5
6
7
8
9

Figure 7. Probability distributions of the change in JJA mean surface O₃ concentrations as a result of tree mortality for grid boxes with low (<10th percentile) baseline NO_x:VOC emission ratios and high (>10th percentile) baseline NO_x:VOC emission ratios. Top: results from mortality-driven changes in emissions only (Simulation 3 – Simulation 1). Bottom: results from mortality-driven changes in emissions and deposition combined (Simulation 4 – Simulation 1).



1
2
3
4
5
6
7

Figure 8. Left: mean JJA mixing ratios of reactive nitrogen oxides in the base scenario (Simulation 1). Right: the relative changes as a result of predicted tree mortality (Simulation 4 – Simulation 1). (A, B) Total NO_y ; (C,D) NO_x ; (E,F) HNO_3 ; and (G,H) the sum of all alkyl-, peroxy-, and acylperoxy-nitrates.



1

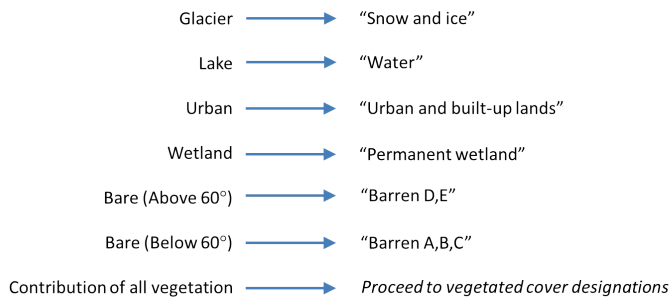
2

3 Figure 9. Left: mean JJA biogenic-SOA surface mass concentrations in the base scenario
4 (Simulation 1). Right: the change in biogenic-SOA mass as a result of predicted tree mortality
5 (Simulation 4 – Simulation 1).

6

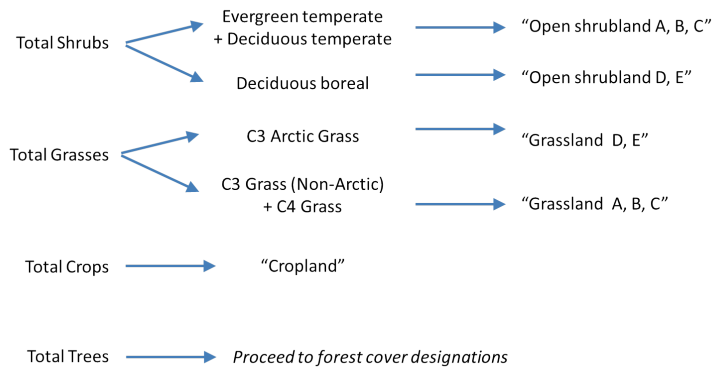
1. LAND COVER DESIGNATION

Determined as which of the following comprises the largest fraction of the grid box.



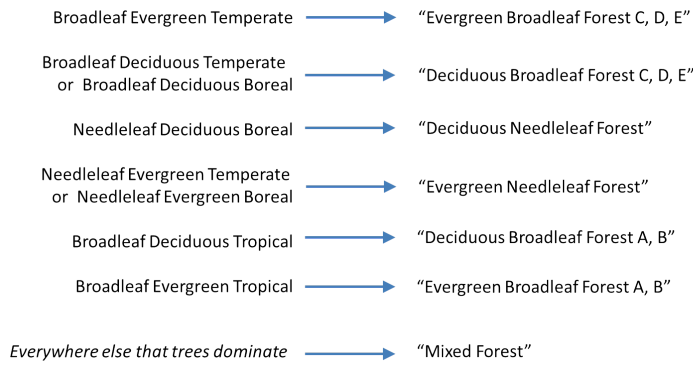
2. VEGETATED COVER DESIGNATION

Determined as which of the following comprises the largest fraction.



3. FOREST COVER DESIGNATION

Determined as which of the following comprise more than 70% of total tree fraction.



1

2

3 Figure A1: Mapping of native CLM land input classes to soil-NO_x biomes (according to

4 Steinkamp and Lawrence, 2011) for land cover harmonization in GEOS-Chem.